NCEP Forecasts of the El Niño of 1997–98 and Its U.S. Impacts

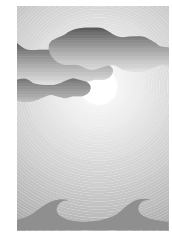

Anthony G. Barnston, Ants Leetmaa, Vernon E. Kousky, Robert E. Livezey, Edward A. O'Lenic, Huug Van den Dool, A. James Wagner, and David A. Unger
Climate Prediction Center, National Centers for Environmental Prediction, National Oceanic and Atmospheric Administration, Camp Springs, Maryland

ABSTRACT

The strong El Niño of 1997–98 provided a unique opportunity for National Weather Service, National Centers for Environmental Prediction, Climate Prediction Center (CPC) forecasters to apply several years of accumulated new knowledge of the U.S. impacts of El Niño to their long-lead seasonal forecasts with more clarity and confidence than ever previously. This paper examines the performance of CPC's official forecasts, and its individual component forecast tools, during this event. Heavy winter precipitation across California and the southern plains–Gulf coast region was accurately forecast with at least six months of lead time. Dryness was also correctly forecast in Montana and in the southwestern Ohio Valley. The warmth across the northern half of the country was correctly forecast, but extended farther south and east than predicted. As the winter approached, forecaster confidence in the forecast pattern increased, and the probability anomalies that were assigned reached unprecedented levels in the months immediately preceding the winter. Verification scores for winter 1997/98 forecasts set a new record at CPC for precipitation.

Forecasts for the autumn preceding the El Niño winter were less skillful than those of winter, but skill for temperature was still higher than the average expected for autumn. The precipitation forecasts for autumn showed little skill. Forecasts for the spring following the El Niño were poor, as an unexpected circulation pattern emerged, giving the southern and southeastern United States a significant drought. This pattern, which differed from the historical El Niño pattern for spring, may have been related to a large pool of anomalously warm water that remained in the far eastern tropical Pacific through summer 1998 while the waters in the central Pacific cooled as the El Niño was replaced by a La Niña by the first week of June.

It is suggested that in addition to the obvious effects of the 1997–98 El Niño on 3-month mean climate in the United States, the El Niño (indeed, *any* strong El Niño or La Niña) may have provided a positive influence on the skill of medium-range forecasts of 5-day mean climate anomalies. This would reflect first the connection between the mean seasonal conditions and the individual contributing synoptic events, but also the possibly unexpected effect of the tropical boundary forcing unique to a given synoptic event. Circumstantial evidence suggests that the skill of medium-range forecasts is increased during lead times (and averaging periods) long enough that the boundary conditions have a noticeable effect, but not so long that the skill associated with the initial conditions disappears. Firmer evidence of a beneficial influence of ENSO on subclimate-scale forecast skill is needed, as the higher skill may be associated just with the higher amplitude of the forecasts, regardless of the reason for that amplitude.

1. Introduction

Until 1997, many oceanographers and meteorologists believed that the El Niño of 1982–83 would probably be the strongest El Niño–Southern Oscillation (ENSO) episode on record in the twentieth century. However, the period of boreal summer 1997 through spring 1998 brought another El Niño of approximately equal intensity. The development and climate impacts of the 1997–98 El Niño were probably more widely anticipated than ever before, as forecasters had several months lead time to predict the climate impacts in the United States for the forthcoming cold season. Greater anticipation was possible for this episode due to advances in observational technology, real-time global monitoring, and dynamical forecasting capability, all

Corresponding author address: Dr. Anthony G. Barnston, NOAA/NCEP, World Weather Building, Room 604, 5200 Auth Rd., W/NP51, Camp Springs, MD 20746-4304.
E-mail: abarnston@ncep.noaa.gov
In final form 20 May 1999.

of which have been aided by substantial increases in computer capacity.

Among the observational advantages achieved in recent decades are the existence of a reliable archive of global outgoing longwave radiation (OLR) since 1979 (Gruber and Krueger 1984), the related development of more accurate satellite-derived precipitation estimates beginning in 1979 (Xie and Arkin 1997), and the creation of the NCEP–National Center for Atmospheric Research (NCAR) global reanalysis datasets for a large variety of global fields since 1958 (Kalnay et al. 1996). While observations of the ocean and atmosphere from the early 1950s to 1979 are satisfactory, those from 1979 to the present are more complete and more accurate. During the 1997–98 El Niño a network of ocean/atmosphere sensors, the Tropical Ocean Global Atmosphere–Tropical Atmosphere–Ocean (TOGA–TAO) array (McPhaden et al. 1998), produced the most detailed observations yet available across the equatorial Pacific.

In addition to observational advancement, our physical understanding of, and ability to predict, ENSO episodes has gradually increased throughout the 1980s and 1990s. In the 1980s, both dynamical and statistical forecast tools were developed. Statistical tools such as filtered composite analysis (e.g., Ropelewski and Halpert 1986, 1996) and canonical correlation analysis (CCA; Barnett and Preisendorfer 1987; Barnston and Ropelewski 1992) were helpful in describing and diagnosing ENSO-based relationships within the increasingly dense global datasets. Dynamical predictive models were also developed in the 1980s, led by the Lamont-Doherty simple coupled model (Cane and Zebiak 1987). While use of statistical models has continued into the 1990s, their growth and demonstrated effectiveness may have reached a relative plateau compared to the more persistent development and performance increases of dynamical models. The use of comprehensive ocean–atmosphere coupled models has been made possible by the emergence of larger, faster computers. As computational power increases, prospects for more sophisticated and accurate dynamical climate forecast models remain bright. Among the most advanced models to date are those of the Center for Ocean–Land–Atmosphere Studies (COLA; Kirtman et al. 1997), the National Centers for Environmental Prediction (NCEP; Ji et al. 1996), and the European Centre for Medium-Range Weather Forecasts (ECMWF; Stockdale et al. 1998). Hybrid statistical–dynamical models have also emerged, such as that used at Scripps Institution of Oceanography (Barnett et al. 1993).

Because of the unusual strength of the 1997–98 El Niño, as well as its early onset in late spring of 1997, the increased arsenal of dynamical model forecast output allowed forecasters to make seasonal outlooks of impacts for the upcoming winter (1997/98) with unprecedented confidence. The main purpose of this paper is to examine this El Niño's impacts on the continental United States, and the accuracy of NCEP's forecasts made for 3-month periods spanning October 1997 to June 1998. Sections 2–4 briefly describe the data and NCEP's prediction tools, as well as NCEP's predictions of the tropical Pacific SST itself. Section 5 summarizes El Niño's expected impact on the climate in the Pacific–North American region. In section 6, Climate Prediction Center (CPC) climate forecasts and the corresponding observations are examined. In evaluating the forecasts, there is some discussion of the unexpected late spring drought in the southern and southeastern United States and its possible association with the manner in which the El Niño dissipated. Section 7 offers some thoughts about the role of the El Niño on medium-range forecasts and their skill. A summary and discussion are given in section 8.

2. Data

This paper uses a variety of atmospheric and oceanic data. The 200-hPa height and winds are from the NCEP–NCAR reanalysis (Kalnay et al. 1996). Global precipitation data, derived both from the Climate Anomaly Monitoring System (CAMS) (Ropelewski et al. (1985) and from OLR, are known as "CAMSOPI'' (Xie and Arkin 1997). The OLR dataset itself is based on the *National Oceanic and Atmospheric Administration-12* Advanced Very High Resolution Radiometer IR window channel measurements by the National Environmental Satellite, Data and Information Service (NESDIS)/Satellite Research Laboratory (Gruber and Krueger 1984). Sea surface temperature (SST) data come from an empirical orthogonal functions reconstruction (Smith et al. 1996) before 1982, and from the optimal interpolation system (Reynolds and Smith 1994) for 1982 and later. Subsurface sea temperatures are derived from an analysis system that assimilates oceanic observations into an oceanic GCM (Behringer et al. 1998). Surface climate in the mainland United States (temperature, precipitation) are from the CAMS for station analyses, and from climate division data from the National Climatic Data Center (e.g., Cayan et al. 1986) in the

analyses for the 1997–98 period. The anomalies of the OLR, CAMPSOPI, and 200-hPa fields are based on the 1979–95 normal period; those of U.S. temperature and precipitation are based on 1961–90, and SST anomalies are based on 1950–79. While the differing base periods introduce minor anomaly misalignment among the fields, this is small compared with the interannual variability related to ENSO.

3. NCEP's climate prediction tools

The climate forecast system at NCEP consists of two broad classes: 1) tools that forecast the tropical Pacific SST, and 2) tools that forecast the U.S. surface temperature and precipitation. The tools used at NCEP for each of these purposes are shown in Table 1. For forecasting the Pacific SST, the NCEP coupled ocean–atmosphere model (Ji et al. 1996) is run with full coupling in the tropical Pacific region. Two statistical models—CCA and constructed analogues (CA)—are also run (O'Lenic 1995). The CCA (Barnston and Ropelewski 1992) uses patterns in the recent global sea level pressure and tropical Pacific SST to predict SST in a number of regions across the tropical Pacific on the basis of historical pattern relationships. The CA (Van den Dool 1994; Van den Dool and Barnston 1995) expresses the current global SST field, and the SST's recent (within previous 1-yr) evolution, as a linear combination of past SST fields over the same recent seasons from historical data. That linear combination is then used to form a weighted average of the subsequent past SST developments, which is used as the forecast. Using the forecasts of the above three models, a statistical consolidation into a single forecast (Unger et al. 1997) is carried out with multiple linear regression, using the historical record of the observations and the forecasts of each model.

For forecasts of U.S. surface climate, ensemble mean forecasts of the *NCEP Coupled Model* are used (Livezey et al. 1996, 1997a). Eighteen individual ensemble members contribute to this mean forecast. These forecasts represent the second of a two-tiered process, the first tier being the tropical Pacific SST forecasts and the second being ensemble integrations of the NCEP GCM using the predicted SSTs from the first tier as boundary conditions. While the forecast SSTs are used to force the atmospheric GCM in the tropical Pacific basin in the second tier, SSTs in the other tropical ocean basins and outside of the Tropics are prescribed as those observed at the initial time, damped toward climatology over a 45-day period. The GCM forecasts are run out to six months, encompassing 3-month periods that begin up to 4.5 months after the run time (i.e., they are centered up to 6 months after run time). Additional input from statistical models is used, including CCA (Barnston 1994), OCN (Huang et al. 1995), and ENSO composites (Livezey et al. 1997b). The *CCA* uses recent patterns of global SST, Northern Hemisphere 700-hPa height, and U.S. temperature or precipitation itself as its predictors. The *OCN* attempts to capture recent low-frequency persistence, or changes in the "normals,'' and consists of a persistence of the mean anomaly of temperature (precipitation) over the last 10 (15) years for the particular season and location. The *ENSO composites* depict the distribution of temperature or precipitation anomalies that have occurred historically in association with warm or cold ENSO episodes, based on the average SST anomaly in the central tropical Pacific (5°N–5°S, 150°W–180°). This relatively small region, straddling the west flank of the Niño 3.4 region, is used because anomalous convection can be induced with smaller SST anomalies than farther east due to the greater climatological warmth west of 150°W. This SST-sensitive region may therefore be more closely related

TABLE 1. Climate forecast tools used at NCEP for predicting tropical Pacific SST and predicting U.S. temperature and precipitation.

Tropical Pacific SST	**U.S. temperature (*T*) and precipitation (*P*)**
NCEP Coupled Model (CMP)	NCEP Coupled Model ensemble forecasts
Canonical correlation analysis (CCA)	CCA using global SST, 700-mb height, U.S. *T* and *P*
Constructed analogues (CA)	OCN: persistence of *T* (last 10 yr) and *P* (last 15 yr)
A statistical consolidation of CMP, CCA, and CA	ENSO composites for *T* and *P* based on historical data
	Soil moisture tool using recent *P* and *T* data

to extratropical teleconnections, despite being somewhat less stable statistically than a larger region would be. The composites are used when a warm or cold episode is in progress or is expected, based on the SST forecasts. A statistical consolidation of the three tools (other than the composites) is made using a scheme similar to multiple regression, to aid the forecasters in objectively combining the input from the several tools. A statistical forecast tool based on *soil moisture* (Huang et al. 1996) is also incorporated at locations and seasons in which it is known to be helpful, such as in large portions of the interior continent in spring and summer.

4. NCEP's SST forecasts during the 1997–98 El Niño

Figure 1 shows the series of forecasts from NCEP's three prediction tools and their final consolidation, along with the corresponding observations, for the SST anomaly averaged over the Niño 3.4 region in the east-central tropical Pacific (5°N–5°S, 120°–170°W) over the period starting in mid-1996 and ending in late 1998. SST forecasts, issued once each month, are shown for each of NCEP's three tools in the first three panels, and for their consolidation in the final panel. The forecasts are for 3-month means centered at the indicated month, except for the coupled model whose forecasts are for 1-month means. Each SST anomaly forecast is shown at 1-month resolution for the 6 months following issuance. The open circles show the 1-month mean observations. The time of forecast issuance is normally near midmonth, or about two weeks later than the time of the most recently observed SST data. The dotted line in Fig. 1 connects the observed SST near the time of issuance to the forecast for one month later. For the two statistical models, the most recent SST data consist of 3-month means ending with the month previous to the month of issuance. This predictor timing was designed to smooth out "noise" to better represent the larger spatial and temporal scales. While this approach may have merit in many climate situations, it implies that the most recent instantaneous SST conditions are not always well represented in the statistical models, especially when the SST is changing quickly. This helps explain why the statistical forecasts lagged the observations during the rapid onset of the El Niño in spring and summer of 1997.

It is evident from Fig. 1 that the three NCEP models all predicted some warming in forecasts made in early 1997. The coupled dynamical model came closest to predicting the rapid growth rate in spring and summer, and the peak magnitude in fall 1997. The coupled model's forecasts from the June through December 1997 initial times were highly accurate, and those made during spring 1997, while somewhat too weak, were clearly suggestive of developing strong El Niño conditions. The CCA was able to predict a high-amplitude SST anomaly only after such an anomaly was reflected in the observed recent 3-month mean SST. The constructed analogue model never reflected the high initial magnitude in its short-lead forecasts, although it attained two-thirds that magnitude in its forecasts from late 1997. Neither the CCA nor constructed analogue forecast a high rate of change of SST in spring 1997. The consolidated NCEP forecast represents a compromise between the skillful forecasts of the coupled model and the relatively amplitude-deficient statistical forecasts. That it did not favor the statistical forecasts (particularly in view of there being two of them) reflects the past performance of each of the three tools, and the moderate historical redundancy between the two statistical tools (Barnston et al. 1994). The dissipation phase of the El Niño in late spring 1998 was best handled by the constructed analogue model and somewhat more sluggishly by CCA and the coupled model. The coupled model showed a tendency to favor warm over cold SST during the 1996-98 period (note its forecasts before and after the 1997–98 El Niño).

The NCEP coupled model's SST forecasts were 1 of 10 or more dynamical and statistical forecast sets issued by various researchers or institutions during 1997–98 (Barnston et al. 1999). Some warming of the SST during 1997 was indicated by many of these other models, but none of them predicted the rapid onset[1] or high magnitude of the event as well as the NCEP coupled model. While a few models verified about as well as the CCA and constructed analogue, some underpredicted the El Niño still more severely. Comprehensive coupled models, such as those of NCEP, COLA, and ECMWF, tended to perform better than the simple coupled dynamical models and

[1]Regarding the rapid onset, it is possible that higher-frequency signals such as the Madden–Julian oscillation (MJO) (Lau and Chan 1986; Jones et al. 1998) and/or westerly wind bursts played a role, as discussed in McPhaden and Yu (1999). However, we have not determined whether the MJO was critical to the NCEP coupled model's behavior in spring 1997.

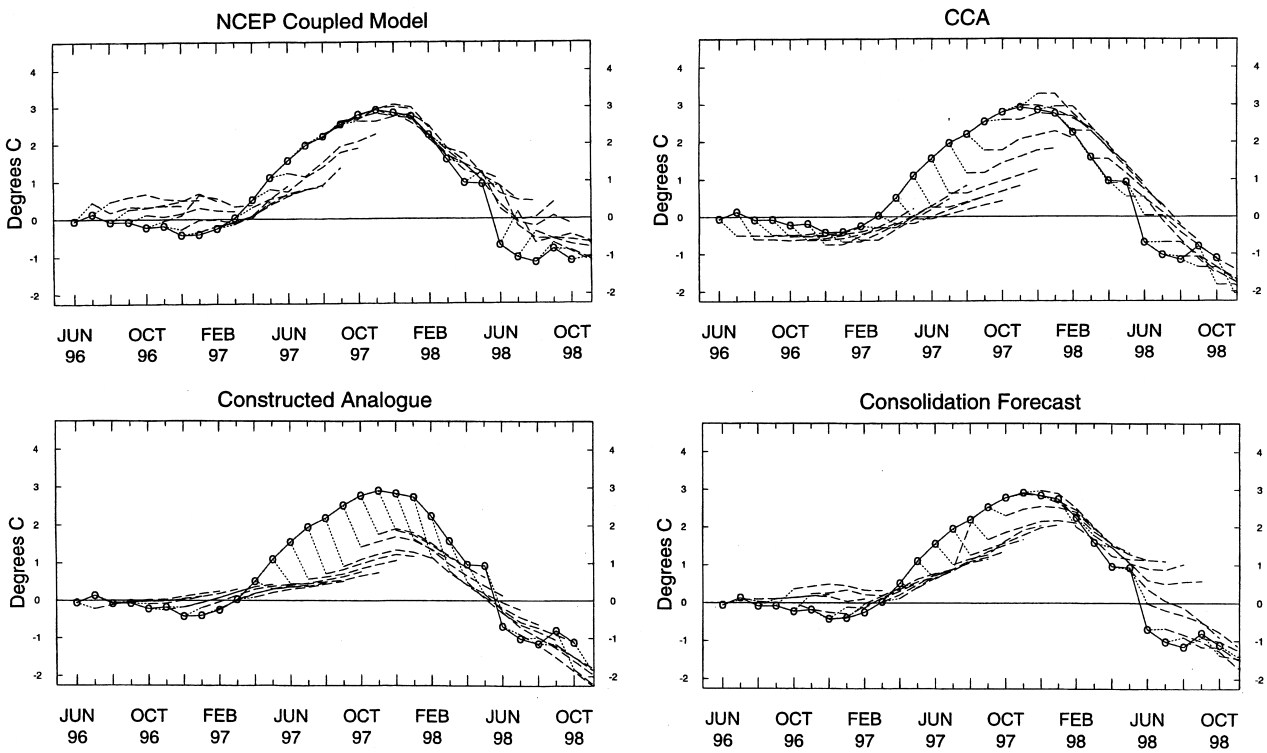

FIG. 1. SST observations and forecasts of the average SST anomaly in the El Niño 3.4 region (5°N–5°S, 120°–170°W) by month, from Jun 1996 to Oct 1998. Forecasts are shown from 1 to 6 months of lead time, for each of NCEP's three tools and their consolidation. Forecasts are for 3-month means centered at the month shown (but are 1-month means for the coupled model). Open circles show the observations at the time of forecast issuance, about 1 to 2 weeks later than the time of the most recently observed SST data. A dotted line connects the observed SST at the time of issuance to the forecast for one month later, and dashed line denotes forecasts at varying lead.

most statistical models during this episode. As an example of two of the best performing dynamical models, the real-time Niño 3 SST forecasts of the NCEP and ECMWF models (Fig. 2) show that the ECMWF model's performance during 1997–98 was also quite good, and perhaps better than NCEP during the early part of 1997. Root-mean-square error (rmse) scores for 5-month lead forecasts verifying from April 1997 through September 1998 are 0.76°C for the NCEP model and 0.86°C for ECMWF. However, for only the April–December 1997 period, representing the growth phase of the El Niño, the ECMWF's rmse is only 0.79°C compared with 0.97°C for NCEP. For 3-month lead forecasts verifying over similar periods, the same qualitative comparative skill results are found, except the two models performed more nearly equally over the entire period (0.50°C for NCEP, 0.49°C for ECMWF).

Figure 3 shows the field of observed SST anomaly across the tropical Pacific basin in December–February 1997/98, and the corresponding forecast made by the NCEP coupled model two seasons in advance in June 1997. The patterns are highly congruent in shape (spatial anomaly correlation is 0.96 over the gridded domain, with 1° latitude by 2° longitude grid resolution). While the forecast was slightly weaker than the observed SST across the central and eastern equatorial Pacific, the forecast provided a clear and believable warning that a strong El Niño, and its attendant global teleconnections and more local U.S.

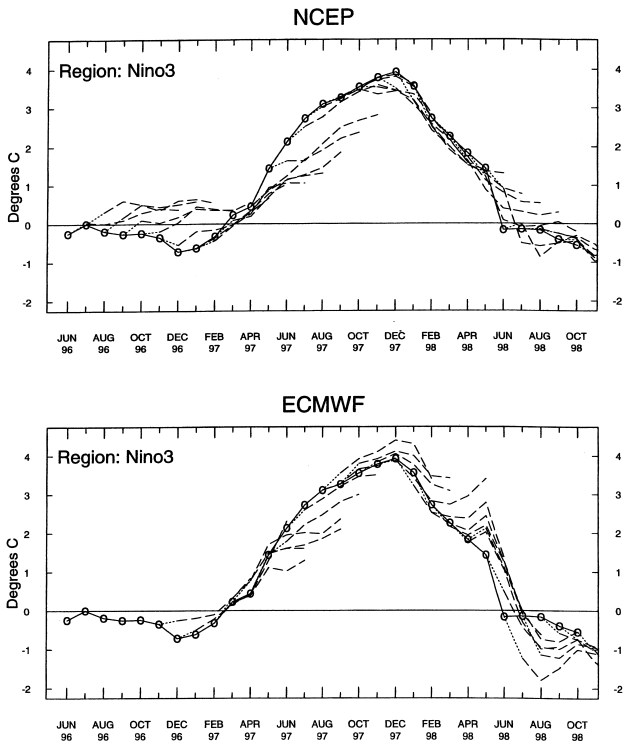

FIG. 2. As in Fig. 1 except for the NCEP coupled model and the ECMWF coupled model, and for the Niño 3 region (5°N–5°S, 90°–150°W).

climate impacts, were in the making for the forthcoming winter. The event had in fact already become strong by June, and the model was indicating further strengthening. Despite the somewhat weaker consolidated forecast due to the deficient indications of the statistical models, the SST for the forthcoming winter was forecast well enough in June 1997 to prompt unequivocal forecasts of U.S. wintertime impacts with ample lead time. As will be shown below, the probability anomalies that were issued in these forecasts strengthened as the summer and fall progressed, making possible an unprecedented degree of public awareness and preparedness.

5. Expected atmospheric effects of positive tropical Pacific SST anomalies

To appreciate how extratropical climate forecasts would be formulated given the presence or expected continuation of an El Niño, we briefly review our understanding of the anomalous features of the general atmospheric circulation induced by the increased heating in the tropical Pacific. [Among others, a recent discussion of this tropical-to-extratropical connection is found in Shukla (1998)]. The anomaly fields of 200-hPa height and winds in the Pacific basin in January–March of the El Niño years of 1983, 1992, 1987, and 1998 are shown in Fig. 4. The 1992 and 1987 cases represent moderately strong El Niños, while the events of 1983 and 1998 were very strong. The heating in the troposphere associated with enhanced deep convection over the warmer-than-normal tropical Pacific SST is most marked in the mid-Pacific (approximately 130°W–180°) where the climatological SST is already close to the 28°C deep convection threshold. The upward motion and atmospheric heating normally found in the far western equatorial Pacific is extended eastward over the enhanced convection. Near and eastward of the maximum of enhanced upward motion, covering approximately 100°–170°W, the weakened trades near the surface and enhanced easterly flow in the upper troposphere produce a subtropical anomalous anticyclonic couplet at 200 hPa in both hemispheres (Arkin 1982), straddling the anomalous easterly equatorial flow (Fig. 4). Although the

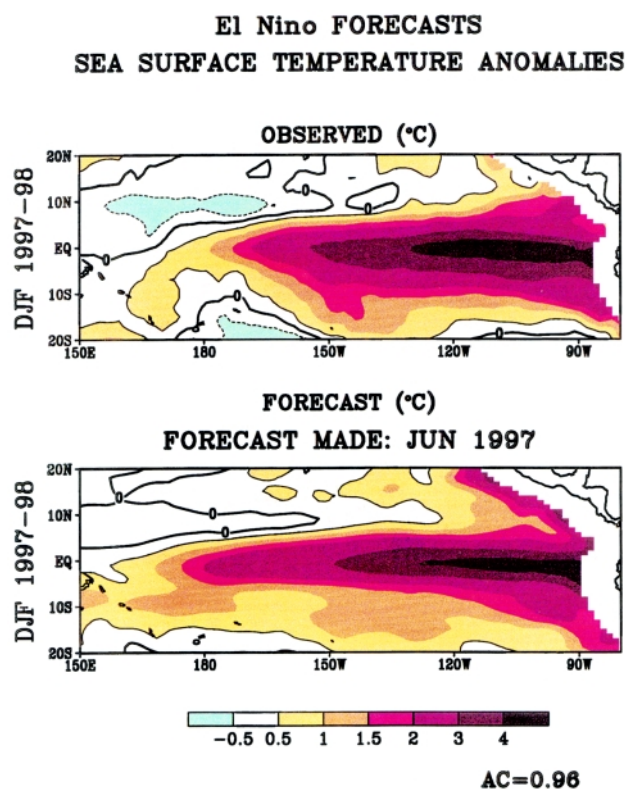

FIG. 3. The SST anomaly field in the tropical Pacific basin in Dec–Feb 1997–98 (top), and the forecast of the anomaly field made by the NCEP Coupled Model in Jun 1997 (bottom). Contour intervals as shown in figure legend. The spatial anomaly correlation between the two panels is shown at lower right.

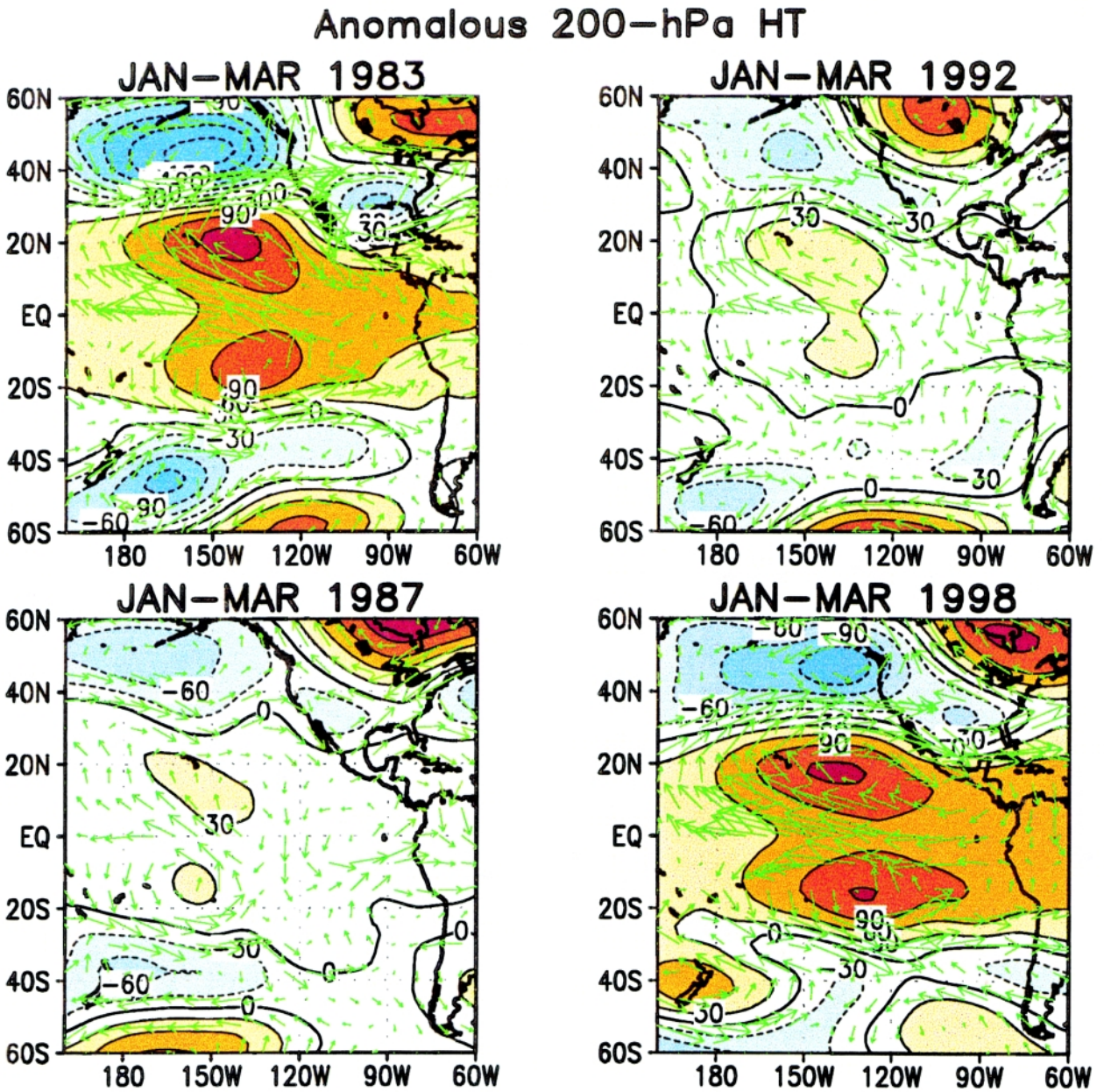

FIG. 4. The 200-hPa height and wind anomaly fields in the Pacific basin in Jan–Mar of 1983, 1992, 1987, and 1998. Contour interval is 30 m; negative contours dashed.

El Niños of 1986–87 and 1991–92 had about two-thirds the east-central equatorial Pacific SST anomaly of those of 1982–83 and 1997–98, the difference in the strengths of the subtropical anticyclonic couplet is proportionately far greater. The teleconnections in the extratropics are also significantly weaker in 1987 and 1992 than in the stronger El Niño cases. On the other hand, the positive 200-hPa anomaly over Canada appears comparably strong in all four cases. The greater intensity of the negative height anomaly south of the Aleutians in 1983 than in 1998 could be a consequence of the more westerly location of the strongest SST anomalies in early 1983 (not shown).

In common to all significant El Niños is an enhanced subtropical Pacific ridge associated with a descending branch of the stronger-than-normal Hadley circulation in both hemispheres, and an anomalous trough at higher latitudes—mainly in the winter hemisphere. At the latitude approximately midway between the subtropical ridge and the midlatitude trough there is an enhanced jet stream and north-to-south temperature gradient, and thus a strengthened storm track. This

structure induces a longwave pattern with downstream features defining the familiar Pacific–North American (PNA) and/or Tropical–Northern Hemisphere (TNH) patterns (Wallace and Gutzler 1981; Barnston and Livezey 1987), including an anomalous ridge over south-central Canada and trough over the Gulf of Mexico and southeastern United States. This overall El Niño–related atmospheric structure (Horel and Wallace 1981) is well represented in nonlinear numerical ocean–atmosphere climate models (Kumar et al. 1996), making possible realistic forecasts of North American climate anomalies attendant to El Niño. Successful representation has also been achieved using linear numerical models (e.g., Ting and Hoerling 1993; Peng and Van den Dool 1999).

In the continental United States, El Niño episodes historically tend to feature a strong subtropical jet stream over the southern part of the country from late fall through winter and much of the following spring, supplying energy and moisture to storms crossing the Gulf of Mexico. Persistent stronger-than-normal low pressure south of the Gulf of Alaska transports mild maritime air inland to the western North American continent, cutting off the supply of cold air for much of western and central Canada and the northern parts of the United States. As a result, El Niño brings cool, wet conditions from the southern plains eastward to Florida and mild weather from the northern Rockies to western New England. There is also some tendency for dryness in the Ohio Valley and over the northern Great Plains, both in association with an enhanced ridge over south-central Canada. Heightened storminess in California occurs with many El Niño episodes, but less reliably than the wetness over the Gulf states. Observations (not shown here) as well as numerical simulations (Hoerling and Kumar 1999) suggest that northern California, as well as Oregon and Washington State, are likely to receive above-normal precipitation during very strong El Niño episodes, while this wetness tends to be more limited to southern and central California during mild to moderate El Niño episodes. The numerical experiments indicate that the details of the West Coast's response are closely related to the location and orientation of the Pacific jet.

The atmospheric effects of El Niño in midlatitude North America are strongest from boreal winter through midspring. Thus, anomalies of 200-hPa height and winds similar to those shown in Fig. 4, except for October–December of the initial year of the four El Niño events (not shown), are much weaker than those three months later, despite equally strong SST anomalies. The 1-month analyses show that these effects start becoming significant in December. This reflects the essential role of the boreal midwinter atmospheric structure (i.e., strong latitudinal temperature gradient, strong Hadley circulation, and strong jets) in activating ENSO's extratropical teleconnection patterns. This required setting helps explain the weakness and inconsistency of extratropical effects in the summer hemisphere.

6. NCEP's forecasts of temperature and precipitation during the 1997–98 El Niño

Beginning in summer 1997, based on existing conditions and the SST forecasts, NCEP/CPC forecasters were confident that a strong El Niño was in place and would persist through the upcoming winter. In effect, a forecast of opportunity presented itself. The forecasters' confidence allowed them to place great weight on the ENSO composite tool (Table 1), although the other tools—particularly the NCEP coupled model forecasts—turned out to be skillful as well. The forecasts of most of the tools were qualitatively similar, although their strengths differed. Even the OCN forecasts, which show just the decadal trend component of the forecast, were skillful, suggesting that the El Niño mapped onto the current interdecadal signal.

a. October–December 1997: A phasing-in of El Niño impacts

The top panel of Fig. 5 shows the NCEP/CPC probability anomaly forecasts of precipitation issued in mid-September, for the October–December 1997 period. The anomalies are given with respect to the 1961–90 climatology, within which the tercile boundaries are defined. The corresponding observations are shown in the bottom panel. The observations are expressed as rankings with respect to the 104-yr period 1895–1998. The verification process, however, uses the tercile definitions based only on 1961–90. Figure 6 presents the temperature forecast and observations in a similar fashion. The El Niño began to influence U.S. weather patterns in fall of 1997 as anomalous wetness affected the Southeast as early as October and central and southern California beginning in November. October and December turned out to be wet also in the central plains, the coast of Texas, and the middle Atlantic portion of the eastern seaboard, as well as Georgia and Florida. Autumn was unusually mild over

the northern plains and along parts of the Pacific coast. This warmth, plus dryness from Montana to the western Dakotas, was likely associated with El Niño. In California, the wetness would continue through winter to early June 1998, resulting in a record number of days with precipitation during the 12-month water year (July–June) at a number of cities.

The skill of the forecasts shown in Figs. 5 and 6 is evaluated using the Heidke skill scores, a rating based on the number of locations at which forecasts are categorically correct in terms of three climatologically equally likely categories, or terciles (below, near, and above normal). The score is zero when the number of correct forecasts equals that expected by chance, and 100 for all-correct forecasts. The appendix provides a more complete explanation of this score. Verification was carried out at 59 approximately equal-area climate divisions. Their locations are roughly collocated with the station network shown in Fig. 1c of Barnston (1994). (In spring 1998, this 59 climate division network was changed to a 102 climate division network for verification.) Figure 7 shows the time series of the Heidke skill for NCEP's 0.5-month lead forecasts for precipitation for 3-month periods from November–January 1995–96 to September–November 1998. Two versions of skill are shown: 1) only for locations forecast as nonclimatology; and 2) for all locations, where those with climatology forecasts are given one-third credit (Van den Dool et al. 1997). The percentage of locations given nonclimatology forecasts is shown at the bottom of Fig. 7. In cases in which all locations are forecast as climatology, the first version of the skill does not exist, and the second version has a Heidke score of zero. Figure 8 shows forecast skill in similar fashion for temperature. For the period October–December 1997, the skill of the precipitation forecast was barely above zero, as only slightly more than one-third of the locations were correctly forecast. While much of the southern tier of states did receive above-normal precipitation, there were serious errors on the smaller-scale aspects of the forecast versus observed pattern. The observations show that a winterlike El Niño impact pattern began setting up in fall, earlier than would normally be expected. The temperature forecast was more successful (Fig. 8), largely because the warmth forecast for the northern plains verified. However, the percentage of the United States given nonclimatology forecasts was small.

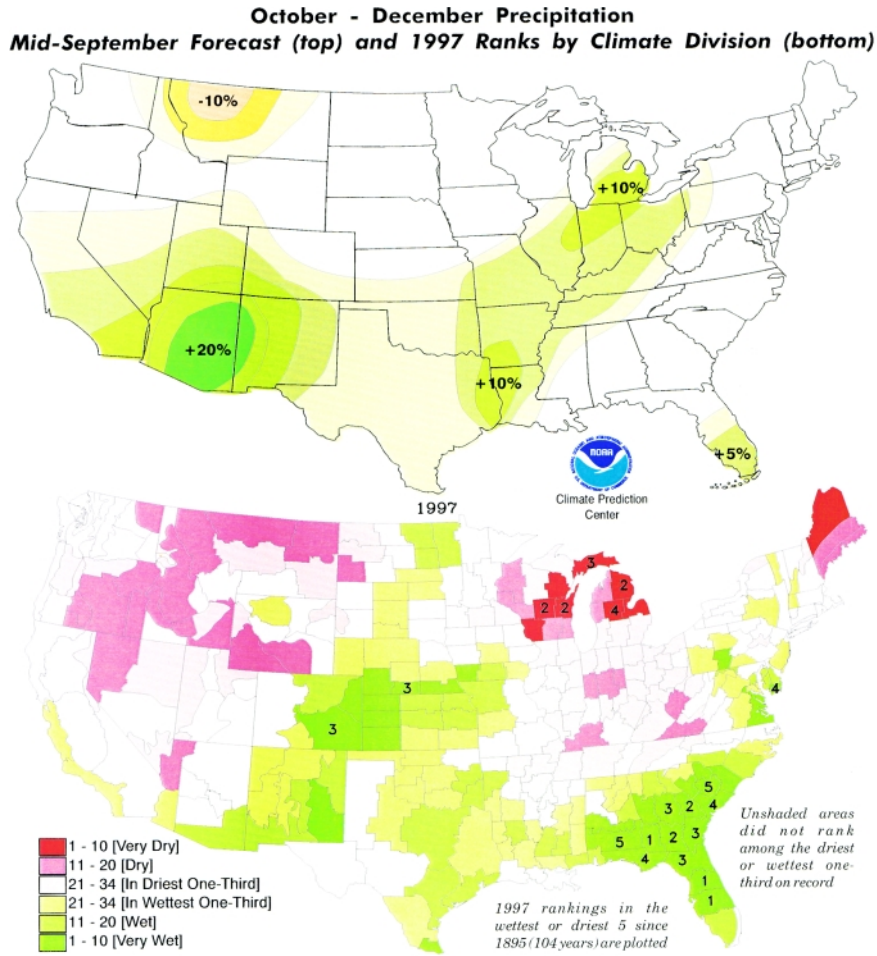

FIG. 5. (top) The forecast of Oct–Dec 1997 precipitation probability anomaly issued by NCEP/CPC in mid-September. Anomalies are with respect to the climatological probability (of 1/3) for the above normal category. Negative anomalies imply equally positive anomalies for the below normal category, and vice versa. (bottom) The observed precipitation outcome is shown in terms of ranking with respect to the 104 years since 1895.

b. January–March 1998: Expected peak time of El Niño impacts

January–March is believed to be the core period for observing El Niño impacts on U.S. weather and cli-

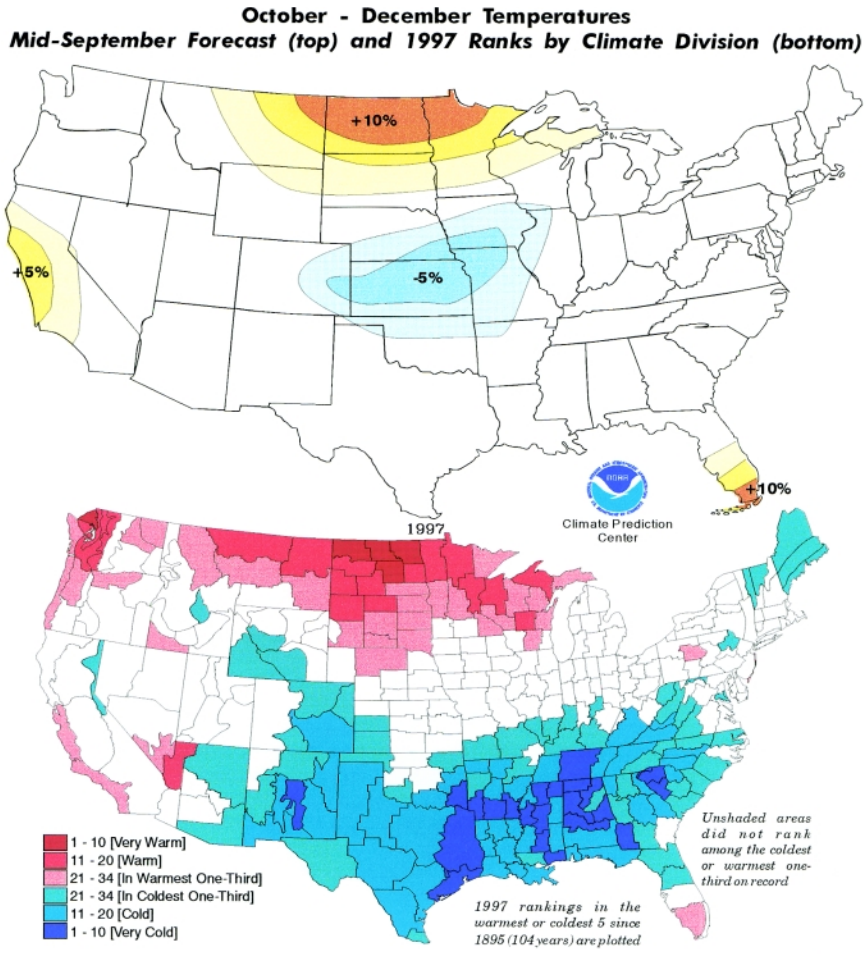

FIG. 6. As in Fig. 5 except for temperature.

mate. This is the case because of the approximately 2-month lag between extremes in the solar cycle and the consequent quasi-stable, roughly steady-state condition established in the seasonally varying ocean-atmosphere system. Thus, the signal-to-noise ratio for North American climate with respect to tropical Pacific SST forcing is maximized in late winter and early spring (Van den Dool 1983; Kumar and Hoerling 1998). This high signal period likely produces the relative maximum in statistical skill in forecasting mean geopotential heights and surface temperature in middle-to-late winter, and the lower skill for forecasts for the single month of December than for any of January, February, or March (Barnston 1994). (However, December–February 1997–98 was most skillfully predicted by CPC in the instance of this El Niño.) The top panel of Fig. 9 shows the NCEP/CPC probability anomaly forecasts of precipitation, issued in mid-December, for the January–March 1998 period. The corresponding observations are shown in the middle panel, and the bottom panel shows the composite forecast tool for El Niño episodes, using historical data from the El Niño years listed above the map. The same set of three maps are shown in similar fashion for temperature in Fig. 10.

The forecasts for January–March precipitation called for abnormal wetness over California, the southern plains, the Gulf coast, and Florida, with above-normal precipitation extending northward into Georgia and South Carolina. Due to forecaster confidence, the magnitudes of the precipitation probability anomalies were unprecedented in the history of U.S. operational seasonal forecasts. As shown in Fig. 9, the final forecast is basically the same as the ENSO composite tool. This is both because that tool was weighted very heavily, and because the indications of the combination of the other tools' forecasts were similar (although somewhat weaker), and where they differed, they were ignored in favor of the composite tool. The 0.5-month lead forecasts, issued in mid-December, indicated probability anomalies of 30% and above for wetness over parts of Kansas, Oklahoma, and Texas, as well as most of the Florida peninsula. Below normal precipitation was forecast with over 30% probability anomalies in the Ohio Valley. In addition, fairly confident forecasts of dryness were issued for Montana. These forecasts turned out to be fairly accurate by climate forecasting standards, with a Heidke score of 29 for the locations assigned nonclimatology forecasts (comprising 73% of all locations), and 21 for all stations. The precipitation forecasts for the December–February period (not shown) were still more skillful, scoring 80 for locations with nonclimatology forecasts and 52 for all locations. The January–March forecast scores were degraded by mainly near normal or wet conditions observed in the Ohio Valley, some dryness and near normal conditions in New Mexico, and above normal precipitation over much of the north-central region.

Nonetheless, the forecasts correctly anticipated wetness in California, the southern plains, and the Gulf coast and Southeast. The wetness extended farther north than expected along the eastern seaboard. Excessive precipitation was particularly extreme in coastal California, Oklahoma, and from Florida westward to southern Louisiana and northward to Virginia. The precipitation in many of these regions ranked in the top 5 of the last 104 years (Fig. 9), and several new records were set. Nationwide, January–March 1998 was the wettest January–March recorded in the last 104 years.

January–March temperatures (Fig. 10) were well above normal across a large part of the country, particularly the northern plains, Midwest, and Northeast, where readings averaged more than 3°C above normal. Nationwide, it was the sixth mildest January–March period in the last 104 years, and the warmest January–February on record. The 0.5-month lead forecast for this period was quite accurate by climate forecasting standards, but, as was the case for precipitation, less accurate than the December–February forecast (not shown). The Heidke score for the nation was 51 for the 73% of locations receiving nonclimatology forecasts, and 37 for all locations. Most of the area in the northern United States was warm as expected, as was the California coast. The forecast did not verify well in southern Texas and the Southeast, where forecasts of negative temperature anomalies were not realized.

While the canonical [e.g., a composite mean, a CCA or joint-

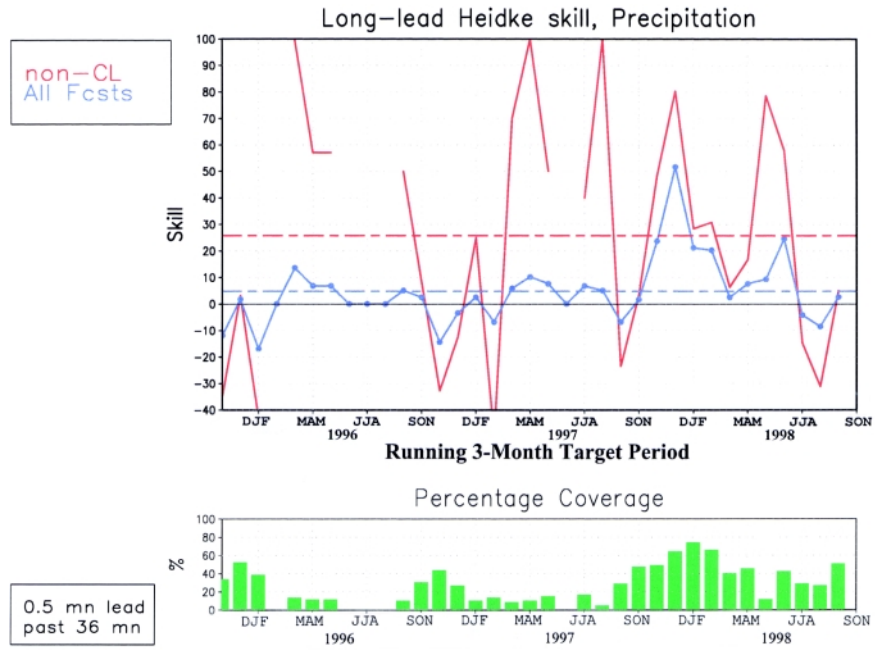

FIG. 7. Time series of Heidke skill scores (see appendix) for 0.5-month lead NCEP/CPC forecasts of precipitation for Nov–Jan 1995 to Sep–Nov 1998. The broken, highly variable line shows skill for only the set of locations given nonclimatology forecasts. When all stations are forecast as climatology, no skill value is given. The less variable line shows skill for all stations, where climatology forecasts are scored as one-third correct (i.e., the chance rate). The means of the scores for each of the two versions of skill are indicated by the horizontal lines across the graph. The percentage of locations given nonclimatology forecasts is shown in the histogram at bottom.

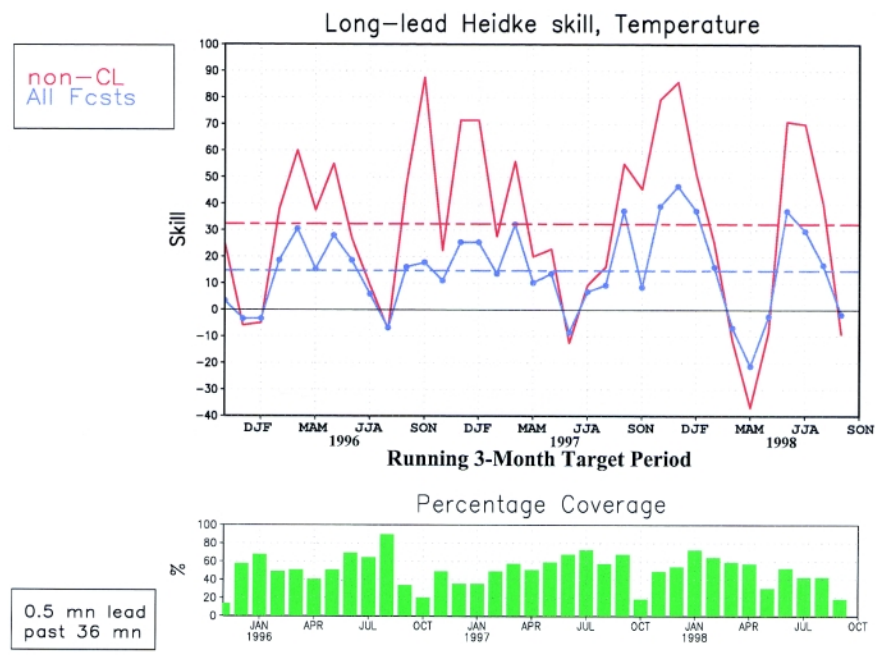

FIG. 8. As in Fig. 7 except for temperature forecasts. Season is identified by middle month in bottom panel.

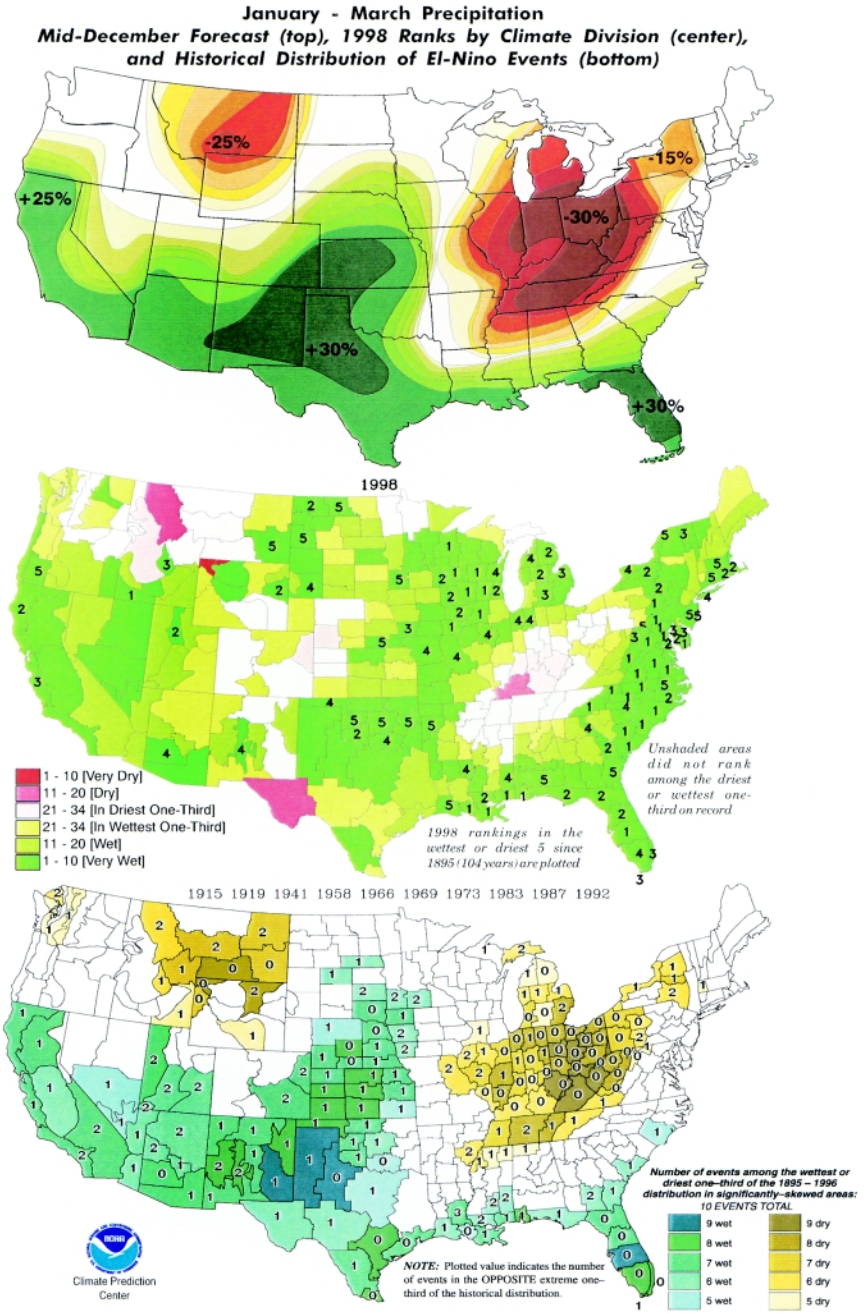

FIG. 9. (top) The forecast of Jan-Mar 1998 precipitation probability anomaly issued by NCEP/CPC in mid-December. Anomalies are with respect to the climatological probability (of 1/3) for the above normal category. Negative anomalies imply equally positive anomalies for the below normal category, and vice versa. (middle) The observed precipitation outcome in terms of ranking with respect to the 104 years since 1895. (bottom) The composite precipitation category frequency pattern derived from the historical data for the El Niño years listed above the map.

EOF mode, or the pattern defined by Ropelewski and Halpert (1986), etc.] climate patterns associated with El Niño are reasonable best guesses for the forecast, it is expected that events related to other climate phenomena (e.g., the North Atlantic oscillation) or of a more random nature relating to the atmosphere's extratropical internal dynamics may result in a somewhat different observed pattern. (The expectation of such deviations is manifested in the variability among ensemble members in atmospheric GCM simulations with prescribed SST forcing, and in the "unexplained variance" parameter in statistical ENSO models.) The fact that the December–February forecasts verified with higher skill than those of January–March is likely related to this random aspect of the atmosphere in 1997–98. Specifically, examination of maps of 1-month mean anomalies at 200 hPa (not shown) indicates that the typical El Niño–related extratropical atmospheric pattern (the PNA/TNH structure) largely broke down in March 1998 and somewhat reestablished itself in April. This March failure is thought to be a random peculiarity of the 1997–98 event.

An additional reason for a superior December–February skill in temperature forecasts is the long-term warming trend found in much of the United States through much of the annual cycle, which tilts the odds against the below normal tercile even in much of the southeastern United States during El Niño winters. (For example, January–March of the recent warm events of 1983, 1987, and 1992 had little or no below normal temperatures anywhere in the United States.) Some of the CPC forecast tools (particularly the CCA) indicated below normal temperature for this region for January–March, implying that the impact of the very strong El Niño would outweigh a decadal temperature trend, despite a clear representation of the trend in the CCA (which, however, did not encompass the Gulf states appreciably in

January–March). While the NCEP temperature forecasts for January–March contained some area that was below normal near the Gulf states, the December–February forecasts did not, resulting in a higher skill score for December–February. One is led to wonder, with the generally upward temperature trend, whether we will see below normal winter temperatures again with El Niño in more than small, isolated areas within the Gulf states. (In the El Niño of the 1950s through 1970s, by contrast, much of the entire southeastern third of the United States tended to be colder than normal.) The central Gulf states have been exempt from the long-term warming trend in winter seen in much of the rest of the United States partly because of the tendency toward more frequent El Niños in the last 20 years, which themselves have favored relative coolness in that area as compared with the remainder of the United States. The causes of global climate changes, seen in multidecadal trends, are not presently known; they may be a combination of the effects of increasing greenhouse gases and aerosols and natural (nonanthropogenic) climate variability. Regardless of their physical causes, at CPC they are "modeled" by the OCN, and in a less exclusive manner by the coupled model, the CCA, and in a set of ENSO composites developed in late 1998 that incorporates linearly fitted trends (not shown here; R. Livezey 1999, personal communication). CPC is attempting to relate atmospheric trends to trends in SST in specific regions, such as the eastern tropical Indian Ocean and western tropical Pacific, and subsequently model them numerically. It is clear that trends can play just as important a role in climate forecasting in North America as ENSO fluctuations.

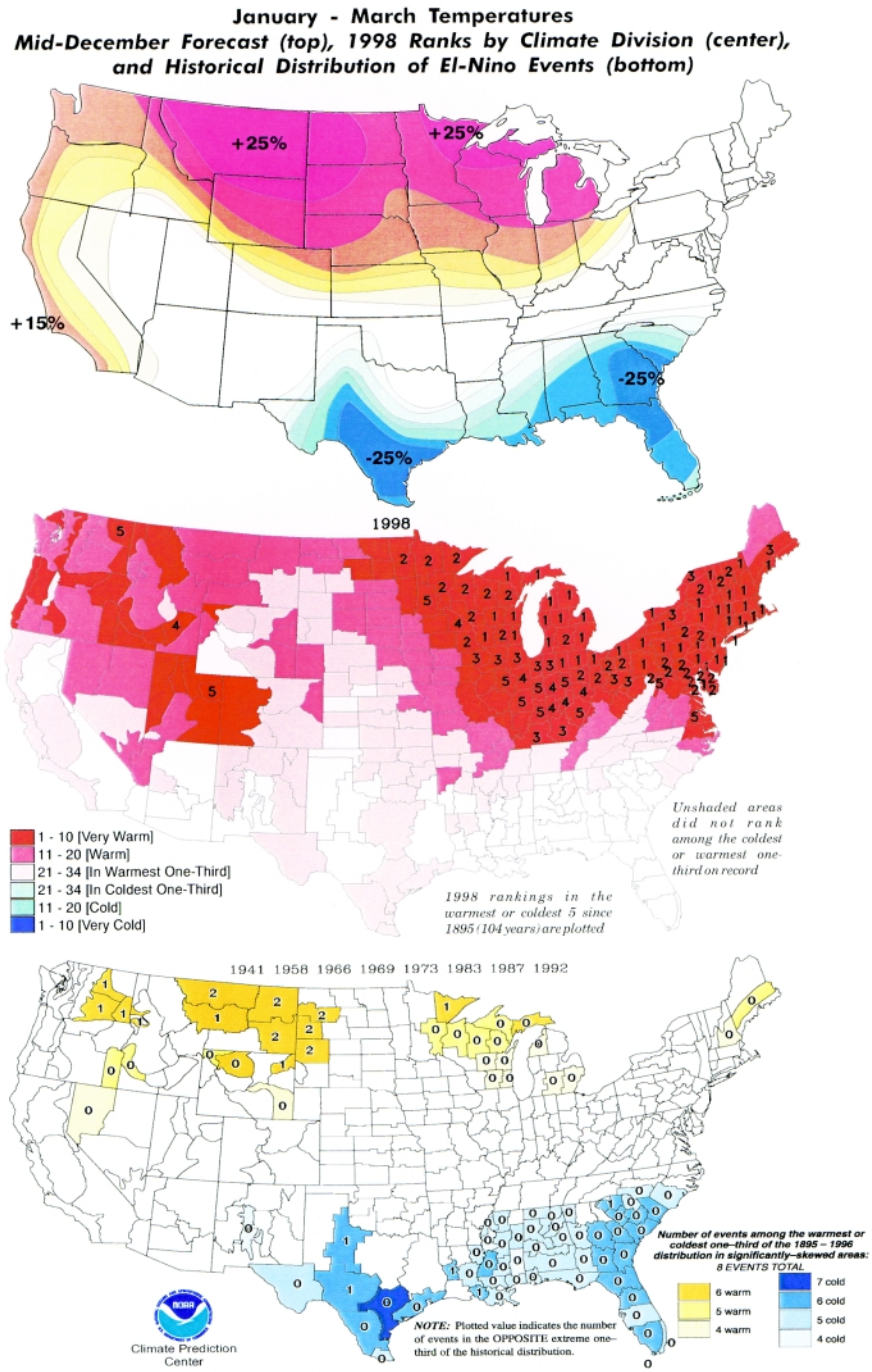

FIG. 10. As in Fig. 9 except for temperature.

Hence, for all seasons from 1995 to early 1998 the OCN has done slightly better than any other individual tools for temperature forecasts (Van den Dool et al. 1999).

The 0.5-month lead precipitation and temperature forecasts of the NCEP coupled model, the CCA, and the OCN for January–March 1998 (made in mid-December) are shown in Fig. 11. The left column of

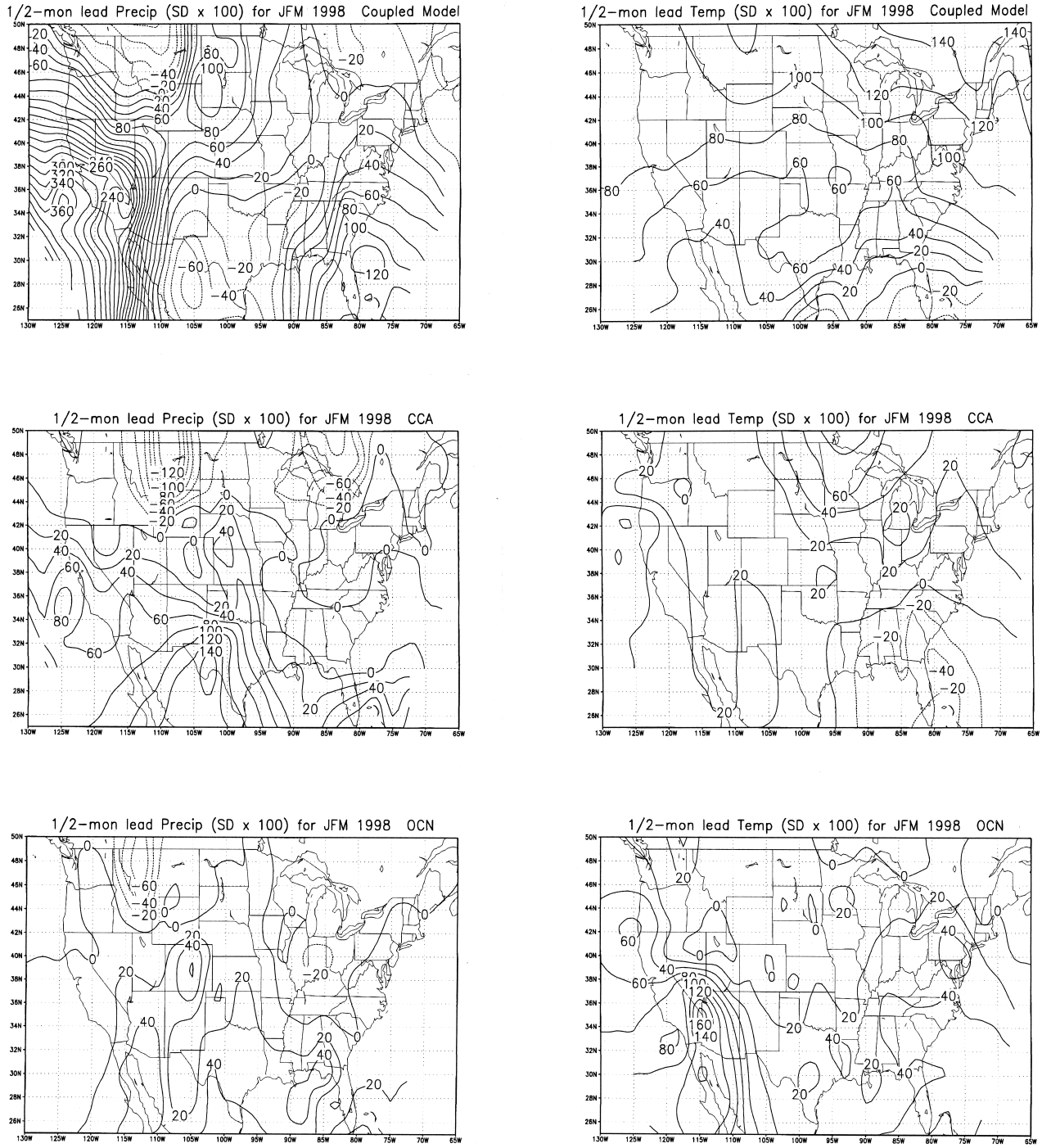

FIG. 11. Forecasts for precipitation for Jan–Mar 1998 made in mid-December (0.5-month lead) from three of the individual tools used by CPC forecasters: the NCEP coupled model, the CCA, and the OCN. Precipitation forecasts are shown in left column, temperature forecasts in right column. Units are standardized anomaly (× 100). Forecasts of the ENSO composite tool are shown at the bottom of Figs. 9 and 10; the soil moisture tool is not shown because it is not used heavily for winter forecasts.

Fig. 11 indicates that the precipitation forecasts of the three tools (other than the ENSO composites) were in very rough agreement (e.g., wetness in the Southwest, Florida, and parts of the central plains; dryness in the northern Rockies), but varied considerably in many ways. The coupled model had by far the strongest forecast, with top one-percentile rainfalls (> 2.5 standard deviations) indicated for south-central California and top quintile rainfall in and near Florida. These regions were given high confidence in the final forecasts, and

verified favorably. The coupled model forecast for dryness centered in southern Texas was overruled by the other tools. The CCA forecast, while having a generally correct pattern, was weak on the above normal precipitation in the Southeast. The OCN scored fairly well for precipitation without "knowing" that an El Niño was occurring; this may be due to the increasing frequency of El Niños (e.g., 1987 1992, 1995), or at least a tilt toward an El Niño–like climate (e.g., 1988, 1990, 1991, 1993, 1994), over the last 15 years. For temperature, the coupled model again verified relatively well, largely because it predicted warmth for all of the United States except for southern Texas and Florida. The OCN also scored well because of its nearly pervasive warm forecast. The OCN's Heidke score, being categorically based, did not suffer at all from the warm "bull's-eye"in the interior Southwest due to strong trends there. Although the CCA is capable of incorporating long-term trends in its forecasts, it missed much credit because of its cool forecast for the Southeast and the smallness of its warmest regions in the north central states and the far West.

Table 2 shows the Heidke scores, for the entire United States, of 0.5-month lead forecasts of the four main individual tools (coupled model, CCA, OCN, and ENSO composites), and of CPC's final forecast (with locations having "CL" given one-third credit), for the running 3-month periods of October–December 1997 to April–June 1998, although the scores for most of the tools were still not computed for spring 1998. Forecasts of the individual tools were "masked out" at locations having cross-validated correlation skill estimates of less than 0.3, so that forecasters only saw portions of the map expected to be minimally skillful. Hence, the forecasters did not see the total maps as they are shown in Fig. 11. The skills of the indi-

TABLE 2. Heidke skills for the forecasts of individual tools, and for CPC's official forecast, during the 1997–98 El Niño. Skill for precipitation forecasts is shown at top, and for temperature forecasts at bottom. The forecasts of the individual tools are scored only at locations having minimal expected skill (see text); other locations are given the default one-third credit. "NA" indicates that the tool's score was not available.

Precipitation							
	Oct–Dec	**Nov–Jan**	**Dec–Feb**	**Jan–Mar**	**Feb–Apr**	**Mar–May**	**Apr–Jun**
Coupled model	2	-1	3	6	9	NA	NA
CCA	3	11	14	9	7	NA	NA
OCN	10	14	9	14	8	NA	NA
ENSO composite	6	11	30	25	13	-4	NA
Official	2	24	52	21	20	2	8
Temperature							
	Oct–Dec	**Nov–Jan**	**Dec–Feb**	**Jan–Mar**	**Feb–Apr**	**Mar–May**	**Apr–Jun**
Coupled model	9	20	34	27	18	NA	NA
CCA	3	8	3	5	-10	NA	NA
OCN	3	34	26	30	5	NA	NA
ENSO composite	0	30	58	28	18	-6	NA
Official	9	39	47	37	16	-7	-21

vidual tools shown in Table 2 are computed only for the locations with this minimal skill level (approximately half of the total area), with the other locations given one-third credit. During the high signal-to-noise conditions that accompany strong ENSO episodes there may be potential for higher skill forecasts than during average climate conditions, and the masking out of the normally lower skill locations may have deprived the forecasters of worthy information. This may be the case particularly for the coupled model, whose skill is concentrated nearly exclusively in responses to ENSO (Livezey et al. 1996). In fact, when the tools are verified over the entire United States for January–March 1998 (Fig. 11), their Heidke scores are higher than those of the masked forecasts (and, in most cases, as high or higher than the score of the official forecast.) This raises questions about the use of a constant mask based on mean historical skill; perhaps the degree of masking should be varied, based on the climate conditions at hand, allowing for "forecasts of opportunity" such as strong ENSO episodes.

Figures 7 and 8 show that NCEP's forecast skill was relatively high during the winter of the 1997–98 El Niño. This is especially true from the point of view of the score for all stations, which reached a maximum during that winter for both precipitation and temperature as compared with the other periods shown. Skills for the smaller set of locations given nonclimatology forecasts were among the most accurate forecasts ever verified. It is noteworthy that the percentage coverage of nonclimatology forecasts for precipitation reached an unprecedented level (maximizing at 73% in January–March) during the 1997–98 cold season, undoubtedly related to the high confidence associated with the opportunity that the strong El Niño afforded the forecasters. This confidence comes, in part, as a result of knowledge, acquired in only the last several years, related to results of ensembles of numerical simulations using both observed and contrived SST patterns as the lower boundary. While statistical models usually described ENSO impacts satisfactorily, the observational data upon which they are totally dependent may not be sufficiently long, reliable, or homogeneous to give excellent results. Good verification data are needed in modeling research; however, long training datasets are not required to design a dynamical model's forecast capability. Ideally, dynamical models should be able to forecast events whose basic characteristics have never been observed historically.

Figure 12 shows the sequence of NCEP/CPC precipitation probability anomaly forecasts for January–March 1998 issued at 3-month intervals from mid-March 1997, at a lead time of 9.5 months, to mid-December 1997, at a 0.5-month lead time. In the first two months of 1997, before a significant El Niño was anticipated, the forecasts for the following winter carried weak probability anomalies. The locations receiving nonclimatology forecasts had indications mainly from the statistical OCN forecasts that describe ongoing interdecadal trends, and to a lesser extent from the CCA, which can also capture trends and had access to data showing a buildup of positive subsurface sea temperature anomalies in the western tropical Pacific (Smith et al. 1995). Even the recent trend on its own resembles El Niño conditions to some extent (Zhang et al. 1997). The SST forecast tools had also been hinting at a reversal of the weak cold (La Niña) conditions of the winter of 1995/96 and again in 1996/97. It is therefore not accidental that forecasts issued before the El Niño's appearance somewhat resemble an El Niño pattern. As 1997 progressed and the prospect of an El Niño became more of a reality by June and July, the U.S. precipitation forecast pattern became more precisely that of the El Niño composite (Fig. 9, bottom). As the enormity of the event became more obvious from late summer to midfall, the magnitude of the probability anomalies increased to levels that were previously unthinkable, especially for precipitation, mainly because of the high weight given to the ENSO composites. It is clear from Fig. 12 that NCEP/CPC's forecast anomaly patterns for winter 1997/98 were consistent for at least seven months prior to the validation time, with increasing confidence as the lead time diminished.

c. April–June 1998: Unpredicted drought in southern/southeastern United States

ENSO impacts are known to continue into the spring season, especially through April, following their strongest manifestations in winter (Livezey et al. 1997a). In the forecasts run in mid-March 1998, the SST forecast models were indicating a dissipation of the El Niño by early summer. It was also understood that late boreal spring is when the climatological SST peaks in the central and eastern tropical Pacific, and has the smallest year-to-year variability, tending to damp or neutralize prespring ENSO-related anomalies. (The late spring is therefore characterized by a minimum in the annual cycle of the persistence of the ENSO condition, and a skill barrier for ENSO prediction.) Therefore, forecasters were progressively lowering the weight given to the El Niño composites for

the spring and early summer 1998 forecasts. The composites themselves are noticeably weaker in late spring than winter. Still, the forecasts showed considerable resemblance to the composites, which differ from their winter counterparts. However, spring and early summer 1998 saw a radical and unexpected change in the climate pattern as a massive dome of high pressure that had been covering portions of northeastern Mexico in winter (against the odds as shown by El Niño composites) moved northward, blocking storm systems from the southern plains and the Southeast. As a result, significant rains became nonexistent in Florida and elsewhere along the Gulf coast in late March, while heavy rains and numerous severe weather outbreaks swept areas to the north from the Midwest to the East Coast. A series of heat waves and fires began to affect Texas in early May and Florida in early June, greatly intensifying the drought. The South recorded its driest and hottest May–June ever, while north-central Florida measured its driest April–June and third warmest April–June ever. Heavy rainfall did not return to Florida until July, and until even later across the rest of the Southeast and southern plains.

The outlooks for April–June 1998 precipitation had only minimal skill (less than 10), and those for temperature were slightly negative. The precipitation forecasts correctly showed wetness for much of the West, but incorrectly extended the wetness southeastward into Texas during a period of intensifying drought. The forecasts also incorrectly indicated dryness in the upper Midwest and northern plains, an area that was largely wet. The forecasts missed the dryness that occurred in Florida and the Gulf states. The April–June temperature forecasts were poor. California and Nevada had below normal temperatures that were not predicted, brought about in part by the large-scale flow pattern associated with the anomalous ridge (and drought) downstream. Above normal temperatures over the Great Lakes and Northeast were mostly in an area having forecasts of climatology. The forecast was somewhat better in the Northwest, where observed warmth from Washington to Montana was within a larger area predicted to be warm. The most serious error occurred in the Texas–Gulf–Florida region, where significant positive temperature anomalies were

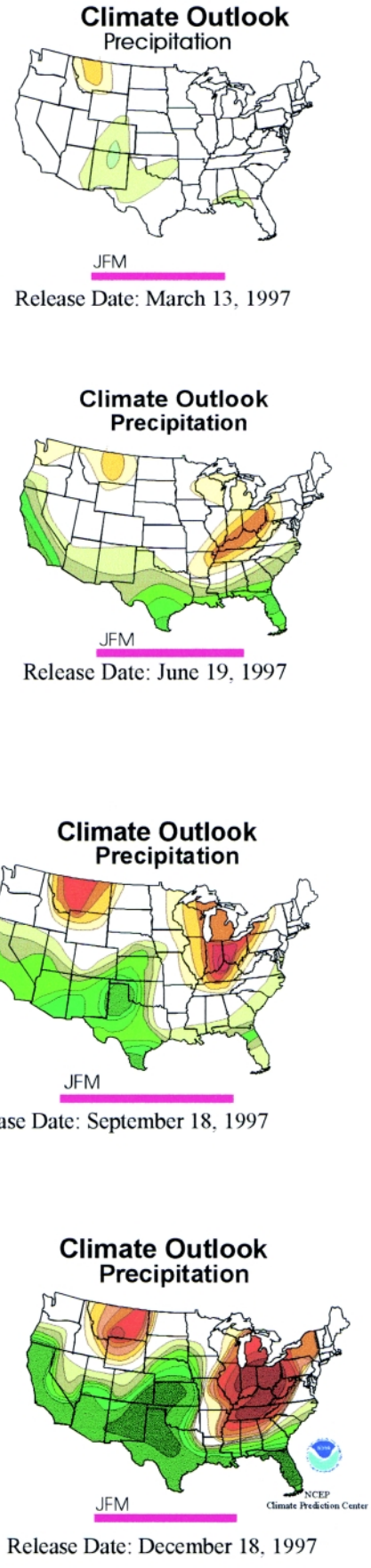

FIG. 12. Sequence of NCEP/CPC precipitation probability anomaly forecasts for Jan–Mar 1998 issued at 3-month intervals from mid-March (9.5-month lead) to mid-December (0.5-month lead) 1997.

observed but the forecast indicated mainly below normal temperatures.

One might reasonably inquire as to why the late spring drought in the South occurred, running counter to the historical El Niño composites. One possibility relates to the particular manner in which the El Niño ended. Although it ended abruptly across much of the tropical Pacific in very late May 1998, the SST in the far eastern tropical Pacific (80°–105°W) remained well above normal throughout the summer. Because the composites are based on the SST in a region farther west, anomalies in the eastern Pacific that conflict with those farther west may induce impacts independent of, and therefore possibly in conflict with, those depicted in the composites. This is especially possible when the eastern anomaly opposes the anomaly farther west, violating the normally strong positive correlation of SST anomalies from South America (except for the 200 km adjacent to the coastline) to the date line. The high SST in the eastern Pacific may have activated the following physical scenario.

As discussed above, in El Niño conditions during boreal winter the subtropical region north of the warm ocean water (e.g., from Hawaii northward to nearly 30°N, and westward to Micronesia) tends to be warm and dry due to an enhanced subtropical upper-atmospheric ridge poleward of the anomalous heating associated with the increased tropical convection and upper-level divergence. During the warm half of the year this atmospheric anomaly pattern is much less pronounced, even with strong SST anomalies (e.g., late boreal summers of 1982 and 1997), due to a weaker north-to-south temperature gradient and thus weaker Hadley circulation and weaker thermal wind on the poleward side of the subtropics. However, the pattern can still appear during the warmer half of the year, especially when the latitudinal temperature gradient is not at its annual minimum from July to September. In late spring 1998, especially June, the twin anticyclones associated with the dying El Niño moved eastward with the convection toward the remaining warm pool just west of South American near 80°–105°W. With the weaker extratropical westerlies typical of late spring, a reduced and more longitudinally localized subtropical atmospheric ridging occurred near (or only slightly downstream of) the longitude of the remaining warm SSTs, such that the subtropical region to the north, in the vicinity of northern Mexico and the south-central United States, experienced above normal temperatures and drought. Because the drought started in late March, before the warm SST became limited to the far eastern Pacific basin, this explanation might be challenged. While it is true that the drought may not have started because of the way in which the El Niño dissipated, it may have persisted as long as it did for that reason. A more detailed diagnosis of this event is given in section 4a(2) of Bell et al. (1999). That diagnosis concludes, in essence, that in late spring 1998 the subtropical ridge in the Northern Hemisphere associated with El Niño moved to the east over North America with the remaining anomalous tropical convection, and migrated northward into the southern United States in association with the normal seasonal solar progression.

The above hypothesis might be supported if it were reproduced by a GCM run using SST boundary conditions prescribed as observed during spring 1998. Figure 13 shows the precipitation anomaly for the April–June 1998 period as observed by CAMS (left) and as simulated by the NCEP coupled model using observed tropical Pacific SST boundary conditions for the same period (right). The simulation is the mean of an 18-member ensemble run. The region inside the contour passed a *t* test at the 95% confidence level for the difference between zero and the ensemble mean. While the model simulation produced a rainfall deficit that was somewhat weak and displaced slightly to the south, the general pattern was correct, lending some support to the hypothesis. The model's underrepresentation may be related to its biases in the location of the subtropical and extratropical ENSO impacts, as described in Smith and Ropelewski (1997), although that study found a mainly westward placement bias. However, Smith and Ropelewski (1997) examined all cases of El Niño collectively, and the April–September period together, possibly hiding the expectations related to the more unique tropical Pacific El Niño SST pattern of late spring 1998, whose timing is also on one end of the 6-month seasonal window. The late spring 1998 case is unusual in that past cases of similar observed SST structure are nonexistent. The recent cases of 1983, 1987, 1992, and even 1993 are similar to the extent that warm water remained in the tropical Pacific through much of the spring, but not in the difference in the dissipation timing between east-central and far-eastern Pacific waters. In midsummer, some observed instances of a tropical Pacific SST pattern similar to that of April–June 1998 do exist and are not found to be associated with a high pressure dome over the South or Southeast. Use of a numerical model may therefore be particularly valuable in this late spring case, providing information

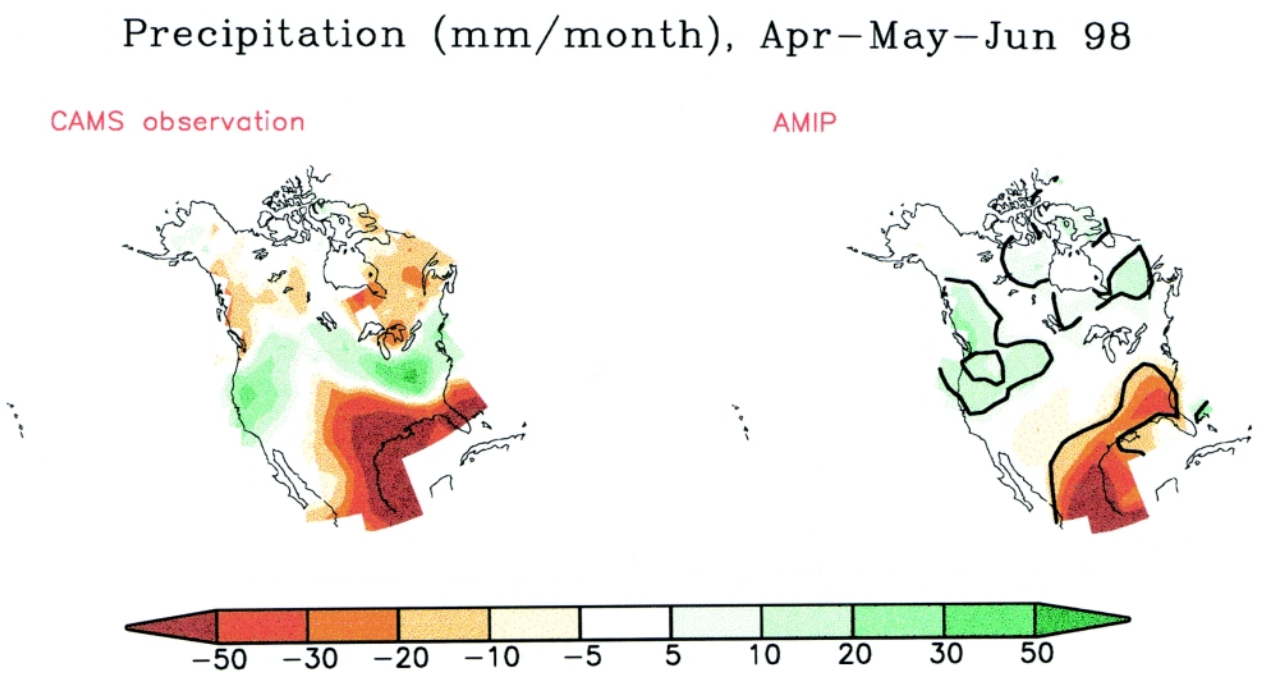

FIG. 13. Precipitation anomaly (mm month^{-1}) for Apr–Jun 1998 as observed (left), and as simulated by the NCEP climate atmospheric GCM using observed tropical Pacific SST boundary conditions for that period (right). An 18-member ensemble was used. Regions statistically significant at the 95% confidence level are contoured.

(subject to some distortion associated with NCEP model biases) unique to this event and not included in Smith and Ropelewski (1997). The benefit of a dynamical model simulation in this instance is the ability to react to forcing situations that do not clearly project on the historical relationships derived from a statistical model developed using long-term data.

7. Suggestions of an ENSO effect on medium-range forecasts and their skill

One of the outcomes of the studies and forecasts made during 1997–98 was the possibility that boundary condition anomalies have visible impacts on the mean weather over 7- or 5-day periods, and even on individual significant weather events. The realization that major boundary condition anomalies may affect medium-range weather has been extended to the issue of attribution in a recent study by Barsugli et al. (1999). In that study, parallel ensembles of simulations of individual large-scale extreme weather events were run for the two cases of 1) observed boundary conditions (e.g., the anomalous tropical SST of the 1997–98 El Niño) and 2) climatological boundary conditions. When the difference between the two ensemble means in the resulting weather developments at medium-range lead times differs significantly in comparison to the ensemble spreads of the two sets of runs, attribution to the anomalous boundary conditions is deemed justified, and the difference regarded as the "synoptic El Niño signal." As discussed in Barsugli et al. (1999), the appearance of boundary condition effects in medium-range weather forecasts requires a lead time sufficiently long for those conditions to begin influencing the forecast, but short enough that the effects of the initial conditions are still reasonably well forecast. This "window of opportunity" is typically in the 5–15-day range. (Note also that during El Niño the initial conditions themselves contain cumulative effects from the El Niño boundary conditions prior to the forecast period.) During periods of anomalous boundary conditions, the combined influences of boundary and initial conditions may increase forecast skill above what it would be without the boundary condition influences. The skills of two such runs using the NCEP medium-range forecast model during the December–February 1997–98 period, for example, have been compared (Fig. 14) at the Climate Diagnostics Center in Boulder, Colorado. While the skill of the model run with climatological SST is indistinguishable from that of the actual SST for the first four days, the benefit of taking the El Niño into account appears from day 5

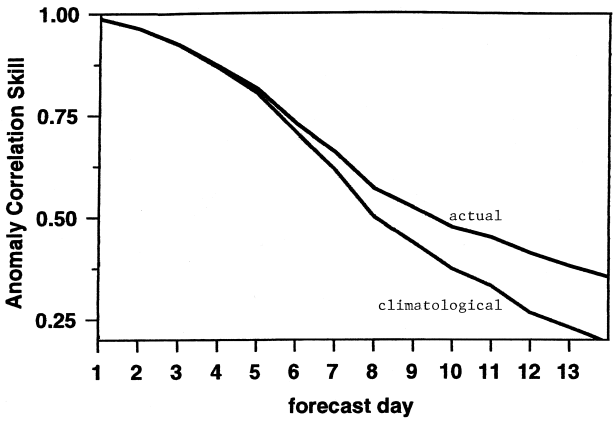

FIG. 14. Forecast skill (as a spatial anomaly correlation) in forecasting 500-hPa height in the PNA region as a function of lead time in the NCEP medium-range forecast (MRF) model with T62 horizontal resolution, run each day during Dec–Feb 1997–98 during the strong El Niño episode. Average skill for the forecast using the actual SST in the tropical Pacific Ocean is shown by the curve having higher skill after 5 days; scores for forecasts using climatological tropical Pacific SST are shown by the other curve. Modeled after Barsugli et al. (1999).

onward and becomes quite visible during the second week of the integration.

On the basis of Fig. 14, one might expect the skill of medium-range forecasts to be somewhat higher during periods of anomalous boundary conditions than near-average boundary conditions. Figure 15 shows the 7-day running mean skill, expressed as a spatial anomaly correlation, of 5-day forecasts of mean 500-hPa height over North America over days 6–10 using NCEP's medium-range forecast model. Over the period from fall of 1997 through part of the winter of 1998/99, a tendency toward increased skill is noted for the El Niño winter of 1997/98 as compared to other portions of the period. In terms of surface temperature forecasts over the United States at this same medium range, Fig. 16 shows month-to-month verification skill (Heidke score) using this same forecast model (modified by human forecasters) for the longer period of 1978 to spring of 1999. The NCEP model has undergone various modifications and improvements during this period. In addition to the gradually increasing skill of the forecasts (note the least squares regression fit to the skill) due to model and observation improvements, the skills for the winter months of December, January, February, and March during five El Niño episodes (1983, 1987, 1992, 1995, and 1998) are highlighted by solid squares, and two La Niña episodes (1989, 1999) by solid circles. Skills of non-ENSO winter months, which are normally slightly higher than those of other seasons, are shown by diamonds. No dramatic or statistically significant skill difference is exhibited during the ENSO winter months: For all 15 non-ENSO winters (60 months) the mean skill is 23.4, while for the 7 ENSO winters it is 28.0 (26.7 for the five El Niño winters, 31.0 for two La Niña winters). Nonetheless, we cannot reject the possibility that the anomalous boundary conditions created by El Niño or La Niña episodes may provide opportunities for forecast skill additional to that associated with the initial conditions alone in forecasts at medium range. As forecast models more correctly simulate anomalies in tropical convection and the impacts of these on global circulations, and as the sample size of cases increases with time, one would hope for firmer real-time evidence of the contribution of boundary forcing to skill in the 615-day range. As stated in Barsugli et al. (1999), however, higher skills may turn out to result from *any* set of forecasts having above-average amplitude, and not just those related to ENSO or, for that matter, related to external forcing.

8. Summary and discussion

NWS/CPC forecasters correctly forecast heavy winter precipitation across California and the southern plains–Gulf coast region for the strong El Niño winter of 1997/98 at least six months in advance. Dryness in Montana and the southwestern Ohio Valley was also correctly forecast. As the winter approached, forecasters increased their confidence in the forecast pattern, and probability anomalies reached record high levels in the months immediately preceding the winter. The warmth across the northern half of the country was also correctly forecast, though the area of warmth extended farther southward and eastward than anticipated. Because the extratropical atmospheric pattern typical of El Niño temporarily broke down in March 1998, forecasts for December–February were more skillful than those of January–March, the opposite of what would normally be expected. The skill of the precipitation forecast for December–February set a new all-time record for CPC's seasonal precipitation forecasts.

The forecasts for the autumn of 1997 showed little skill for precipitation, although the temperature forecasts had fairly good skill. Forecasts for spring 1998 were poor, as a circulation pattern developed that did not conform to the historical El Niño pattern, especially for temperature. It is suggested that this pattern,

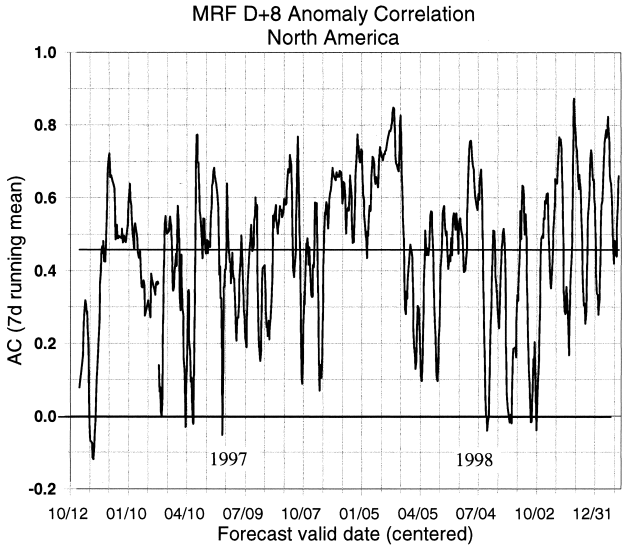

FIG. 15. The 7-day running mean skill of 5-day 500-hPa height forecasts for the 6–10-day range. Skills are shown for mid-October 1996 to early February 1999 and are expressed as a spatial anomaly correlation. The mean skill is indicated by the horizontal line near 0.46 correlation.

related to an unexpected drought in the southern and southeastern states, may have been related to the unique manner in which the El Niño ended. In particular, significant residual warm SST that remained in the far eastern tropical Pacific in May and June may have moved the normally expected El Niño–related subtropical ridge eastward over the Americas, and this ridge may have migrated northward to 25°–35°N with the seasonal solar progression. Simulations of the NCEP medium-range forecast (MRF-12) model using observed SST forcing were able to roughly reproduce this late-spring drought. Similarly localized SST forcing in midsummer has *not* been observed to be associated with such a circulation pattern. Indeed, the circulation pattern broke down by July 1998 despite the persisting positive SST anomalies in the far-eastern tropical Pacific. This may be the case because, during midsummer, the north-to-south temperature gradient, and thus the general Hadley circulation, becomes too weak to sustain the subtropical ridge and higher-latitude trough structure that would appear in response to El Niño, especially when the tropical heating is more limited and localized as it was in the far eastern tropical Pacific in midsummer 1998.

An impact of the anomalous boundary conditions associated with El Niño on medium-range NWP forecasts is suggested in the skills of ensemble simulations that ignore those boundary conditions versus those that take them into account. An increment in the skill of NCEP's medium-range model forecasts has been observed during ENSO winters (but is not statistically significant) over the last two decades. When parallel ensemble simulations are performed with and without the anomalous boundary conditions with respect to an observed extreme large-scale weather event, the issue of attribution to the boundary conditions may be addressed quasi-objectively. Hence, a recent study (Barsugli et al. 1999) attempted to assess the attributability of several extreme weather events during winter 1997/98 to the strong El Niño.

The skillful winter 1997/98 forecasts issued by CPC, while partly a result of the strong ENSO signal provided by nature, may also be attributed to an increasing reliance upon numerical models as input to CPC's forecasts of forthcoming tropical Pacific SST conditions as well as resulting climate impacts over the United States. The success of the forecasts of the International Research Institute of El Niño's global climate impacts during winter 1997/98 (Mason et al. 1999) may be explained similarly. Accommodation of nonlinearity in the ocean–atmosphere climate system is one reason that dynamical models would be expected, ideally, to outperform their linear statistical model counterparts. It has become clearer that El Niño and La Niña are not each others' close opposites (Kumar and Hoerling 1998), and the impact patterns of El Niño may differ somewhat as a function of the event's strength (Hoerling and Kumar 1999) despite being linearly proportional to strength to first order (Kumar and Hoerling 1997). Linear models, such as

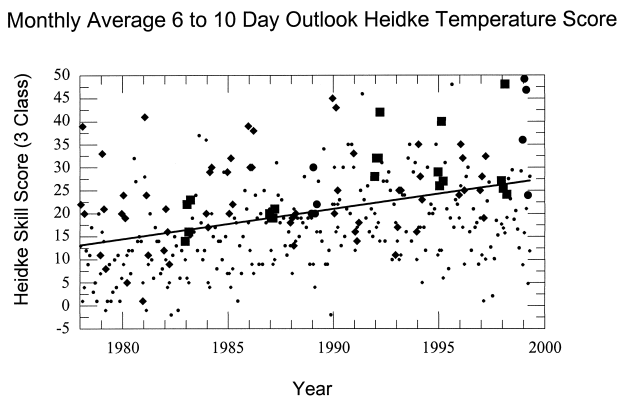

FIG. 16. Monthly mean of the Heidke skill of 5-day mean temperature forecasts for the 6–10-day range. Skills are shown for Jan 1978–Dec 1998. Skills for Dec, Jan, Feb, and March of non–El Niño winters are shown by diamonds; skills for those months of El Niño episodes (1983, 1987, 1992, 1995, and 1998) are shown by solid squares, and La Niña episodes (1989, 1999) by solid circles. A least squares regression fit to all skills is indicated by the straight line.

the harmonic dial method used by Ropelewski and Halpert (1986) or the CCA method (Barnett and Preisendorfer 1987; Barnston 1994), blend the impacts of El Niño episodes of varying strengths in their historical training samples. While the use of multiple modes in CCA and other empirical techniques can partially resolve nonlinearities (and thereby reduce amplitude damping that would result when using one blended mode), dynamical models are comparatively unlimited in this respect. The beneficial use and acceptance of dynamical model forecasts present many challenges, such as the interpretation of ensemble distributions, and recognition and correction of systematic errors. Many of these issues will be more easily addressed as computers become increasingly powerful. The question of predictability, or the upper bound of expected forecast skill given a "perfect" climate model and unlimited computer resources, remains open. Thus, we hope that significant upside potential still exists for dynamical approaches. In the meantime, while we are becoming increasingly comfortable letting dynamical tools influence our operational forecasts, we continue to run statistical models for "reality checks" and for skill benchmarks.

Acknowledgments. Richard Tinker produced the graphics for the ENSO composites, as shown in Figs. 9 and 10. Douglas Le Comte helped write a narrative summary of NCEP's forecast verifications that contributed to section 6. Ming Ji, Arun Kumar, and Wanqui Wang coordinated the reliable and timely production of NCEP coupled model forecasts. Arun Kumar and Wanqiu Wang performed the significance test on the NCEP model's forecasts and simultaneous simulations (e.g., Fig. 13). Assistance with the graphics was provided by Robert Churchill, Wanqiu Wang, Jonathan Hoopingarner, Arun Kumar, Yuxiang He, and Paul Sabol. Alvin J. Miller, Masao Kanamitsu, and Sidney Katz provided valuable in-house reviews of this paper. The three official reviewers provided much valuable additional criticism.

Appendix: The Heidke Skill Score

The Heidke skill score is a measure of forecast accuracy that is widely used when the forecasts and their corresponding observations are expressed as categories (e.g., below normal, near normal, etc.) rather than in numerical form. The score is based simply on the number of forecasts whose category turned out to be correct. The skill (S) formula is $S = 100(C - E)/(N - E)$, where C is the number of locations correctly forecast, E is the number expected to be correct by chance, and N is the total number of locations forecast. For three climatologically equally likely categories (below, near, and above normal), as used by NWS/CPC, E equals $N/3$. Thus, the formula reduces to $S = 100[C - (N/3)]/(2N/3)$. An equivalent way to write this formula is $S = 100 \times 1.5[(C/N) - 0.333]$. Using this formula, a set of all-correct forecasts results in a score of 100, while a set of forecasts with as many correct as would be expected by chance scores 0. Negative scores are also possible, with a lower limit of $-100/(K-1)$ for the case of no correct forecasts, where K is the number of equally likely categories. For the three-category system used at NCEP/CPC the lower limit is −50. The category definitions applied to the NWS/CPC forecasts do not take the probability anomalies into account; rather, all locations having positive probability anomalies are placed into the "above normal" category, and likewise for negative probability anomalies. Occasionally a "near normal" is forecast. The skill is assessed in two ways (Van den Dool et at. 1997): in the first way, locations having the "climatology" forecast are not counted at all, so that only locations for which a categorical forecast is assigned are considered, effectively reducing the value of N. The second scoring method counts all locations, but assigns one-third credit (i.e., the chance hit rate) to locations having climatology forecasts. The second scoring method produces scores that have the same sign as scores from the first method but that are closer to zero in proportion to the fraction of locations having climatology forecasts. Specifically, if the fraction of locations having *non*climatology forecasts is denoted by f, the skill score using the second method equals the skill score using the first method, multiplied by f.

There are benefits and liabilities associated with each of the two methods of assessing skill. The method that only considers locations for which nonclimatoloy forecasts are made has the advantage of rating skill only where the forecasters believed, a priori, that they had ample information and knowledge to warrant making a forecast. Its disadvantage is that it may result in small sample sizes, causing high forecast-to-forecast skill variability. (Consider the extreme case of making a forecast for only one location, in which the outcome would be a Heidke skill score of either −50 or 100.) Another possibly negative characteristic is that a good forecast for a small fraction of locations is credited just as much as a good forecast for a large fraction of locations. The method that gives one-third credit for locations having climatology forecasts always keeps the full sample size and thus has less variable skill results. Assuming that skill

generally averages above zero, it exacts a penalty for making climatology forecasts (but not as severe a penalty as for making incorrect nonclimatology forecasts); it does not give the forecaster any credit for knowing in advance where not to make a forecast. In this presentation we show both skills in order that our readers may decide which is more meaningful for their purposes.

References

Arkin, P. A., 1982: The relationship between interannual variability in the 200 mb tropical wind field and the Southern Oscillation. *Mon. Wea. Rev.,* **110,** 1393–1404.

Barnett, T. P., and R. Preisendorfer, 1987: Origins and levels of monthly and seasonal forecast skill for United States surface air temperatures determined by canonical correlation analysis. *Mon. Wea. Rev.,* **115,** 1825–1850.

——, M. Latif, N. Graham, M. Flugel, S. Pazan, and W. White, 1993: ENSO and ENSO-related predictability. Part I: Prediction of equatorial Pacific sea surface temperatures with a hybrid coupled ocean–atmosphere model. *J. Climate,* **6,** 1545–1566.

Barnston, A. G., 1994: Linear statistical short-term climate predictive skill in the Northern Hemisphere. *J. Climate,* **7,** 1513–1564.

——, and R. E. Livezey, 1987: Classification, seasonality and persistence of low-frequency atmospheric circulation patterns. *Mon. Wea. Rev.,* **115,** 1083–1126.

——, and C. F. Ropelewski, 1992: Prediction of ENSO episodes using canonical correlation analysis. *J. Climate,* **5,** 1316–1345.

——, and Coauthors, 1994: Long-lead seasonal forecasts—Where do we stand? *Bull. Amer. Meteor. Soc.,* **75,** 2097–2114.

——, M. H. Glantz, and Y. He, 1999: Predictive skill of statistical and dynamical climate models in SST forecasts during the 1997–98 El Niño episode and the 1998 La Niña onset. *Bull. Amer. Meteor. Soc.,* **80,** 217–243.

Barsugli, J. J., J. S. Whitaker, A. F. Loughe, P. Sardeshmukh, and Z. Toth, 1999: Effect of the 1997/98 El Niño on individual large-scale weather events. *Bull. Amer. Meteor. Soc.,* **80,** 1399–1411.

Behringer, D. W., M. Ji, and A. Leetmaa, 1998: An improved coupled model for ENSO prediction and implications for ocean initialization. Part I: The ocean data assimilation system. *Mon. Wea. Rev.,* **126,** 1013–1021.

Bell, G. D., M. S. Halpert, C. F. Ropelewski, V. E. Kousky, A. V. Douglas, R. C. Schnell, and M. E. Gelman, 1999: Climate assessment for 1998. *Bull. Amer. Meteor. Soc.,* **80** (May), S1–S48.

Cane, M., and S. E. Zebiak, 1987: Prediction of El Niño events using a physical model. *Atmospheric and Oceanic Variability,* H. Cattle, Ed., Royal Meteorological Society Press, 153–182.

Cayan, D. R., C. F. Ropelewski, and T. R. Karl, 1986: *An Atlas of United States Monthly and Seasonal Temperature Anomalies December 1930–November 1984.* NOAA–U.S. Climate Program Office, 244 pp.

Gruber, A., and A. F. Krueger, 1984: The status of the NOAA outgoing longwave radiation data set. *Bull. Amer. Meteor. Soc.,* **65,** 958–962.

Hoerling, M. P., and A. Kumar, 1999: Understanding and predicting extratropical teleconnections related to ENSO. *El Niño and the Southern Oscillation Multi-Scale Variations, Global and Regional Impacts,* H.F. Diaz and V. Markgraf, Eds., Cambridge Press, in press.

Horel, J. D., and J. M. Wallace, 1981: Planetary-scale atmospheric phenomena associated with the Southern Oscillation. *Mon. Wea. Rev.,* **109,** 813–829.

Huang, J., H. M. Van den Dool, and A. G. Barnston, 1995: Long-lead seasonal temperature prediction using optimal climate normals. *J. Climate,* **8,** 809–817.

——, ——, and K. P. Georgakakos, 1996: Analysis of model-calculated soil moisture over the United States (1931–1993) and applications to long-range temperature forecasts. *J. Climate,* **9,** 1350–1362.

Ji, M., A. Leetmaa, and V. E. Kousky, 1996: Coupled model predictions of ENSO during the 1980s and 1990s at the National Centers for Environmental Prediction. *J. Climate,* **9,** 3105–3120.

Jones, C., D. E. Waliser, and C. Gautier, 1998: The influence on the Madden–Julian oscillation on ocean surface heat fluxes and sea surface temperature. *J. Climate,* **11,** 1057–1072.

Kalnay, E., and Coauthors, 1996: The NCEP/NCAR 40-Year Reanalysis Project. *Bull. Amer. Meteor. Soc.,* **77,** 437–471.

Kirtman, B. P., J. Shukla, B. Huang, Z. Zhu, and E. K. Schneider, 1997: Multiseasonal predications with a coupled tropical ocean global atmosphere system. *Mon. Wea. Rev.,* **125,** 789–808.

Kumar, A., and M. P. Hoerling, 1997: Interpretation and implications of the observed inter–El Niño variability. *J. Climate,* **10,** 83–91.

——, and ——, 1998: Annual cycle of Pacific–North American seasonal predictability associated with different phases of ENSO. *J. Climate,* **11,** 3295–3308.

——, ——, M. Ji, A. Leetmaa, and P. Sardeshmukh, 1996: Assessing a GCM's suitability for making seasonal predictions. *J. Climate,* **9,** 115–129.

Lau, K.-M., and P. H. Chan, 1986: The 40–50 day oscillation and the El Niño/Southern Oscillation: A new perspective. *Bull Amer. Meteor. Soc.,* **67**, 533–534.

Livezey, R. E., M. Masutani, and M. Ji, 1996: SST-forced seasonal simulation and prediction skill for versions of the NCEP/MRF model. *Bull. Amer. Meteor. Soc.,* **77,** 507–517.

——, ——, A. Leetmaa, H. Rui, M. Ji, and A. Kumar, 1997a: Teleconnective response of the Pacific–North American region atmosphere to large central equatorial Pacific SST anomalies. *J. Climate,* **10,** 1787–1820.

——, R. W. Tinker, and A. Leetmaa, 1997b: What will El Niño bring? ALERT transmission, Summer–Early Fall 1997, 20 pp. [Available from Chris Crompton, Ed., 10852 Douglass Rd., Anaheim, CA 92806.]

Mason, S. J., L. M. Goddard, N. E. Graham, E. Yulaeva, L. Sun, and P. A. Arkin, 1999: The IRI seasonal climate prediction system and the 1997/98 El Niño event. *Bull. Amer. Meteor. Soc.,* **80,** 1853–1873.

McPhaden, M. J., and X. Yu, 1999: Genesis and evolution of the 1997–98 El Niño. *Science,* **283,** 950–954.

——, and Coauthors, 1998: The Tropical Ocean–Global Atmosphere (TOGA) observing system: A decade of progress. *J. Geophys. Res.,* **103,** 14 169–14 240.

O'Lenic, E., 1995: A new paradigm for production and dissemination of the NWS's long lead-time seasonal climate outlooks. *Proc. 19th Annual Climate Diagnostics Workshop,* College Park, MD, U.S. Dept. of Commerce, NOAA, 408–411.

Peng, P., and H. Van den Dool, 1999: The impact of 1997/98 El Niño on the mid-latitude atmospheric circulation as evaluated by a steady state linear model. *Proc. 23d Annual Climate Diagnostics and Prediction Workshop,* Miami, FL, U.S. Dept. of Commerce, NOAA, 78–81.

Reynolds, R. W., and T. M. Smith, 1994: Improved global sea surface temperature analyses using optimum interpolation. *J. Climate,* **7,** 929–948.

Ropelewski, C. F., and M. S. Halpert, 1986: North American precipitation and temperature patterns associated with the El Niño/Southern Oscillation (ENSO). *Mon. Wea. Rev.,* **114,** 2352–2362.

——, and ——, 1996: Quantifying Southern Oscillation–precipitation relationships. *J. Climate,* **9,** 1043–1059.

——, J. E. Janowiak, and M. S. Halpert, 1985: The analysis and display of real-time surface climate data. *Mon. Wea. Rev.,* **113,** 1101–1106.

Shukla, J., 1998: Predictability in the midst of chaos: A scientific basis for climate forecasting. *Science,* **282,** 728–731.

Smith, T. M., and C. F. Ropelewski, 1997: Quantifying Southern Oscillation–precipitation relationships from an atmospheric GCM. *J. Climate,* **10,** 2277–2284.

——, A. G. Barnston, M. Ji, and M. Chelliah, 1995: The impact of Pacific Ocean subsurface data on operational prediction of tropical Pacific SST at the NCEP. *Wea. Forecasting,* **10,** 708–714.

——, R. W. Reynolds, R. E. Livezey, and D. C. Stokes, 1996: Reconstruction of historical sea surface temperatures using empirical orthogonal functions. *J. Climate,* **9,** 1403–1420.

Stockdale, T. N., D. L. T. Anderson, J. O. S. Alves, and M. A. Balmaseda, 1998: Global seasonal rainfall forecasts using a coupled ocean–atmosphere model. *Nature,* **392,** 370–373.

Ting, T., and M. P. Hoerling, 1993: Dynamics of stationary wave anomalies during the 1986/87 El Niño. *Climate Dyn.* **9,** 147–164.

Unger, D., A. Barnston, H. Van den Dool, and V. Kousky, 1997: Consolidated forecasts of tropical Pacific SST in Niño 3.4 using two dynamical models and two statistical models. *Experimental Long-Lead Forecast Bulletin,* A. Barnston, Ed., Climate Prediction Center, National Weather Service, U.S. Department of Commerce, Vol. 6, No. 1, 58–60. [Available from CPC, World Weather Building, 5200 Auth Rd., Room 604, Camp Springs, MD 20746-4304.]

Van den Dool, H. M., 1983: A possible explanation of the observed persistence of monthly mean circulation anomalies. *Mon. Wea. Rev.,* **111,** 539–544.

——, 1994: Searching for analogues, how long must we wait? *Tellus,* **46A,** 314–324.

——, and A. G. Barnston, 1995: Forecasts of global sea surface temperature out to a year using the constructed analogue method. *Proc. 19th Annual Climate Diagnostics Workshop,* College Park, MD, U.S. Dept. of Commerce, NOAA, 416–419.

——, and Coauthors, 1997: 1st annual review of skill of CPC long lead seasonal predictions. *Proc. 21st Annual Climate Diagnostics Workshop,* Huntsville, AL, U.S. Dept. of Commerce, NOAA, 13–16.

——, and Coauthors, 1999: 3rd annual review of skill of CPC real time long lead predictions. *Proc. 23d Annual Climate Diagnostics and Prediction Workshop,* Miami, FL, U.S. Dept. of Commerce, NOAA, 9–12.

Wallace, J. M., and D. S. Gutzler, 1981: Teleconnections in the geopotential height field during the Northern Hemisphere winter. *Mon. Wea. Rev.,* **109,** 784–812.

Xie, P., and P. A. Arkin, 1997: Global precipitation: A 17-year monthly analysis based on gauge observations, satellite estimates, and numerical model outputs. *Bull. Amer. Meteor. Soc.,* **78,** 2539–2558.

Zhang, Y., J. M. Wallace, and D. S. Battisti, 1997: ENSO-like interdecadal variability: 1900–1993. *J. Climate,* **10,** 1004–1020.